On the Right Jump Tail Inferred from the VIX Market*

Zhenxiong Li†, Xingzhi Yao‡, Marwan Izzeldin §

November 3, 2022

Abstract

This paper addresses the role of the right jump tail under the risk-neutral measure, as a proxy for fear-of-fear, in the return predictability implicit in the VIX market. A simulation establishes that the right jump tail dominates the left jump tail in explaining various risk measures and their associated term structures. Using VIX futures and options from 2006 until 2020, the superior predictive power for futures returns afforded by the variance-of-variance risk premium ($VVRP$) is shown to arise predominantly from the right jump tail risk. A separate consideration of the continuous and jump tail components of the $VVRP$ outperforms the alternative models in an out-of-sample forecasting exercise and generates non-trivial economic value, especially over short horizons. However, the impact of right jump tail is weak on option returns and only evident for short maturities, suggesting that the fear component cannot be the sole factor explaining the observed losses incurred on the delta-hedged VIX options.

Keywords: Jump tail risk; return predictability, variance risk premium, VIX derivatives

JEL Classification: C15; C32; G15

*The second author (Xingzhi Yao) acknowledges financial support from the Natural Science Foundation of the Jiangsu Higher Education Institutions of China (21KJB630005). We thank Gerry Steele for helpful editorial suggestions and the participants of the CFE 2021 Conference and the RES 2022 Annual conference for insightful discussions.

†Address: Department of Economics, Dongwu Business School, Soochow University, China; E-mail: zxli@suda.edu.cn

‡*Corresponding author.* Address: International Business School Suzhou (IBSS), Xi'an Jiaotong-Liverpool University, 215123, China; Phone: +86 0512 81883243. E-mail: Xingzhi.Yao@xjtlu.edu.cn.

§Address: Department of Economics, Lancaster University, LA1 4YD, UK

1 Introduction

Investor sentiment and asset market volatility are often captured by the VIX index which is published by the Chicago Board Options Exchange ($CBOE$). Derived by the cross section of SPX options, the VIX nonparametrically approximates the expected future index volatility over the next 30 days. Since the VIX is not a directly tradeable instrument, futures and options, subsequently introduced by the $CBOE$ in 2004 and 2006, provide investors with tradeable exposure to volatility. A fast growing recent literature concentrates on measuring and modelling the volatility-of-volatility ($VVIX$) implied by the VIX options due to its crucial role in asset pricing (see Park (2015), Huang et al. (2019) and Yuan (2021), among others).

As indicated by Park (2015) and Huang et al. (2019), investors dislike volatility-of-volatility risk and are willing to pay a premium for downside protection. This indicates that the $VVIX$ contains information, not only on a physical expectation of future volatility-of-volatility risk, but also on its associated risk premium. The latter is defined as the difference between the physical and risk-neutral variances of the VIX index, the so-called variance-of-variance risk premium ($VVRP$) in the work of Kaeck (2018). Despite widespread interest in the variation of the volatility-of-volatility and its risk premia, little progress is apparent in understanding the tail risk manifest in VIX options. The current paper seeks to fill this void by examining the impact of jump tails upon the dynamic properties of the $VVIX$ and $VVRP$ and their predictive power for future returns. Given that the VIX is often referred to as the "investor fear gauge", the $VVIX$ based on the VIX options might be considered the "fear-of-fear". In the present paper, we argue that the right jump tail variation from the VIX option data is attributable to the genuine fear-of-fear component; and that fear per se may account for much of the predictive power underlying the $VVRP$. Disentangling the part of the $VVRP$ associated with normal sized price variations, from that associated with extreme tail events, is likely to provide a better guide to investment decisions.

The main contributions are twofold. First, we assess the role of the fear-of-fear component in return predictability for the VIX market as implied by the $VVIX$, $VVRP$ and their term structures. We follow Bollerslev, Todorov, and Xu (2015) in treating the difference between the left and right jump tail risk premia as a proxy for fear-of-fear, since it is virtually exempt from any compensation for temporal variation in jump tail risk. To ensure the robustness of our predictability results, we conduct both in-sample and out-of-sample analysis while considering various time horizons and pricing factors as control variables.

Second, we identify the different impact of upward and downward jump risk premia on the $VVIX$ and $VVRP$. For this, we undertake a Monte Carlo simulation based upon an extended model of VIX dynamics, as considered in Park (2016). Using simulated VIX options, we also evaluate the contributions to the $VVIX$, $VVRP$ and their associated term structures of the risk-neutral left and right jump tails while justifying the use of the latter as an approximation for the fear-of-fear. The right jump tail depends solely on deep short-lived OTM call options that are worthless in the absence of any substantial increase in the VIX before the options expire. We therefore view this as compensation for exposure to sudden downside movements in the market. With a wide range of strikes and equal numbers of the OTM calls and puts, our simulation study is less prone to the problem of measurement errors, as encountered by the empirical work where bias in the estimation of the left jump tail is induced by frequent misses of VIX deep OTM puts.

The simulation evidence indicates that, for the same magnitude of jump risk premium, the upward jump premium has greater impact than its downward counterpart, on the properties of the $VVIX$ and $VVRP$. Moreover, that impact tends to increase as the jump risk premium increases; and it declines with longer investment horizons. As the upward jump premium increases, it delivers a steeper slope of term structures for the $VVIX$ and $VVRP$. However, changes in the downward jump premium leave the shape of the term structure virtually unaffected. The dominant role played by the upward jump premium is indicative of the superiority of the right jump tail under the risk-neutral measure. The latter approximates the difference between the downward

and upward jump risk premia for large sized jumps. Indeed, regardless of the size of the jump risk premium, the right jump tail clearly outperforms its counterpart in explaining the $VVRP$, $VVIX$ and their term structures.

In the empirical study, we first explore the predictive power of the $VVIX$, $VVRP$ and other traditional predictor variables for VIX futures returns. We establish that the $VVRP$ serves as the top performer for monthly and quarterly return predictions. Moreover, the predictive information underlying the $VVRP$ cannot be fully subsumed by other traditional predictors that we have considered. To disentangle the true source of the return predictability and to characterize the role of the fear-of-fear, we then deprive the $VVRP$ of the right jump tail component. This substantially reduces the R^2 relative to the regression based on the $VVRP$ alone. Finally, a considerable increase in the degree of predictability is achieved when the diffusive and the right jump tail risk components of the $VVRP$ are included as separate predictors. It is also worth noting that the right jump tail remains statistically significant when the traditional predictor variables are included. Our results suggest that the fear-of-fear component proxied by the right jump tail variation is the primary source of the in-sample predictive ability inherent in the $VVRP$ for VIX futures returns.

Out-of-sample results further confirm the in-sample results regarding the role of the right jump tail in return predictions. We show that the $VVRP$ significantly outperforms the historical average model in most of the forecasting horizons and its forecasting power considerably weakens, if not disappears, when the right jump tail component is removed. In addition, the best forecasting performance over short horizons is obtained when the right jump tail is reintroduced to the predictive regression based on the diffusive component of the $VVRP$. Results of the Clark and West (2007) test indicate that such superiority afforded by the right jump tail still remains even after other traditional predictor variables are added in the forecasting exercises. From an asset allocation perspective, we further devise a trading strategy for a mean-variance investor and provide evidence that the right jump tail is nontrivial in generating economic gains, especially

over short horizons.

For the VIX options, we show that over all strike and maturity combinations, OTM delta-hedged VIX options have significantly negative returns. Consistent with earlier studies of Mencía and Sentana (2013) and Park (2015), compared with the $VVRP$, we find that the $VVIX$ is a more significant risk factor affecting VIX option returns. When the $VVIX$ is stripped of the right jump tail variation, a decline in return predictability is only observed for short-dated options. Furthermore, the inclusion of the right jump tail risk does not alter the sign and statistical significance of the coefficients for the $VVIX$. Our results indicate that, while the fear-of-fear proxy plays an important role, it cannot fully explain the negative delta-hedged returns and that the predominant forecast power is afforded by the $VVIX$.

Our work is related to several recent papers that examine the forecasting power of the tail risk measures obtained from SPX options. Bollerslev, Todorov, and Xu (2015), Andersen, Fusari, and Todorov (2015), Andersen, Fusari, and Todorov (2020) and Andersen, Todorov, and Ubukata (2021) show that the return predictability implied by the variance risk premium (VRP) arises largely from the left jump tail, and that this hinges on the SPX deep out-of-the-money (OTM) put options. We build on this literature by constructing the jump tail measure in the VIX market and evaluating its role in the predictions of the VIX futures and option returns. Among the few studies of jump dynamics for the VIX derivatives, Park (2016) emphasizes the importance of upward jumps in pricing performance and Park (2015) and Huang et al. (2019) include jumps as control variables in predictive regressions for VIX option returns. Neither formal treatment of the jump tail risk underlying the VIX market, nor a thorough analysis of jump tails in the VIX return predictability, are to be found in the literature.

Finally, our results enrich the literature on the forecasting performance afforded by the $VVRP$. Despite the extensive study of volatility-of-volatility risk in recent years, empirical work dedicated to the predictability inherent in the $VVRP$ is rather limited. This contrasts sharply with mounting evidence on the usefulness of the VRP as a predictor for aggregate stock market returns, see,

Bollerslev, Tauchen, and Zhou (2009), Drechsler and Yaron (2010), Bollerslev et al. (2014), and Li, Izzeldin, and Yao (2020), among others. Given that investors' aggregate risk aversion could vary differently with the time horizon, Li and Zinna (2018) and Bardgett, Gourier, and Leippold (2019) further establish that the VRP term structure contains additional information on future returns. In contrast, we are among the first to investigate the predictive power of the $VVRP$ and its term structure for VIX futures returns. To improve the reliability of the predictability results, we adopt the IVX approach of Kostakis, Magdalinos, and Stamatogiannis (2015) to account for the potential presence of strong persistency and endogeneity in the variables.

The rest of the paper proceeds as follows. We present our construction of the $VVIX$, $VVRP$ and the jump tails in section 2. A simulation study on the role of jump tail risk is demonstrated in section 3. Section 4 details the data used in our study and section 5 discusses the main empirical results. Section 6 concludes.

2 Construction of Risk Measures

We first derive the risk-neutral expectation of the quadratic variation for the VIX index. We then construct the realized variance for the VIX and obtain the variance-of-variance risk premium as the wedge between the conditional expectations of quadratic variation under the risk-neutral and objective measures. Finally, we extract the investors' fear-of-fear component as proxied by the special compensation for jump tail risk.

2.1 Implied variance measure

The VIX index offers a model-free and market-determined estimate of one-month stock market volatility implied by index option prices. Britten-Jones and Neuberger (2000) and Jiang and Tian (2005) indicate that the VIX can be derived from the prices of S&P 500 call and put options covering a range of strikes. In practice, the published VIX adopts a few approximations due to

the availability of options data.

In the present paper, we calculate the implied volatility of volatility by applying the same method as the VIX to a cross-section of the VIX options. The squared $VVIX$ that captures the model-free implied volatility of VIX futures reads

$$VVIX^2_{[t,t+\tau]} = \frac{2e^{rf\tau}}{\tau}\left[\int_0^{F_t} \frac{1}{K^2} P_t(\tau, K)dK + \int_{F_t}^{\infty} \frac{1}{K^2} C_t(\tau, K)dK\right] \tag{1}$$

where rf is the risk-free rate, F_t is the VIX futures price, K denotes the strike price, τ is time-to-maturity measured in annual units and $P_t(\tau, K)$ ($C_t(\tau, K)$) denotes the price of OTM put (call) options on the VIX. In the subsequent analysis, we always consider the use of squared $VVIX$, thus the $VVIX^2$ notation, unless otherwise stated. To approximate the integral on the right-hand side of equation (1), we follow a procedure that is now adopted as common practice in the related literature: a) interpolate between listed strikes employing a simple cubic spline; b) extrapolate the observed implied volatilities by assuming a flat implied volatility function beyond the available strike prices. To reduce measurement errors induced by the limited availability of strike prices, we generate a grid of strikes with one-point increments and consider strikes covering a range of three times the standard deviation around the futures price.

2.2 Variance-of-variance risk premium

Next, we characterize the variance-of-variance risk premium ($VVRP$) in the form of a gap between the objective and risk-neturalized expectations of the total quadratic variation for the VIX index over a fixed maturity. This premium represents compensation demanded by investor for the risk associated with fluctuations in the return variation of the volatility index.

Following Barndorff-Nielsen and Shephard (2002) and Kaeck (2018), we obtain the realized variance over the interval from t to $t+\tau$ below

$$RVVIX_{[t,t+\tau]} = \frac{252}{n}\sum_{i=1}^{n}\left(\log\left(F_{t_i,t+\tau}\right) - \log\left(F_{t_{i-1},t+\tau}\right)\right)^2 \tag{2}$$

where $F_{t,t+\tau}$ denotes the futures contract on day t with fixed maturity $t+\tau$. For each time horizon τ, the daily return is calculated between two points in the partition $[t,\ t+\tau]$, where $t+\tau$ is the expiry date of VIX options in the following month and t is the trading day after the expiry date of the present month. Since VIX futures maturities are consistent with the expiry dates of the options, this approach achieves exact matching of information in the measurement of the two expectations of the future return variation of the VIX. To capture the premium that investors require to hold variance-sensitive assets, we construct the $VVRP$ as follows

$$\begin{aligned} VVRP_{t,\tau} &\equiv E_t^P\left(QV_{[t,t+\tau]}\right) - E_t^Q\left(QV_{[t,t+\tau]}\right) \\ &\approx RVVIX_{[t,t+\tau]} - VVIX^2_{[t,t+\tau]} \end{aligned} \tag{3}$$

where $QV_{[t,t+\tau]}$ is the quadratic variation measuring the return variation of the log-price process over t and $t+\tau$, $E_t^P\left(QV_{[t,t+\tau]}\right)$ and $E_t^Q\left(QV_{[t,t+\tau]}\right)$ respectively correspond to the objective and risk-neutral expectations of $QV_{[t,t+\tau]}$.

2.3 Jump tail risk

As indicated in Bollerslev, Todorov, and Xu (2015) and Andersen, Todorov, and Ubukata (2021), $VVRP_{t,\tau}$ in equation (3) can be decomposed into a part associated with variation in the diffusive volatility process and a part that is induced by jumps. Define the left and right jump variation under the risk-neutral measure as $LJV^Q_{[t,t+\tau]}$ and $RJV^Q_{[t,t+\tau]}$, their counterparts under the physical measure are therefore $LJV^P_{[t,t+\tau]}$ and $RJV^P_{[t,t+\tau]}$. Specifically, $LJV^Q_{[t,t+\tau]}$ and $RJV^Q_{[t,t+\tau]}$ ($LJV^P_{[t,t+\tau]}$ and $RJV^P_{[t,t+\tau]}$) can be understood as the predictable component of the quadratic variation associated with large negative and large positive jumps under the risk-neutral $Q-$(physical $P-$) measure. By analogy with the definition of $VVRP_{t,\tau}$, the left and right jump tail risk premia can by given by

$$LJP_{t,\tau} = E_t^P\left(LJV^P_{[t,t+\tau]}\right) - E_t^Q\left(LJV^Q_{[t,t+\tau]}\right) \tag{4}$$

and

$$RJP_{t,\tau} = E_t^P\left(RJV_{[t,t+\tau]}^P\right) - E_t^Q\left(RJV_{[t,t+\tau]}^Q\right) \tag{5}$$

where $LJP_{t,\tau}$ is the component of $VVRP_{t,\tau}$ due to large negative jumps and $RJP_{t,\tau}$ is the component of $VVRP_{t,\tau}$ due to large positive jumps.

Consistent with the work of Bollerslev, Todorov, and Xu (2015), we assume that the jump intensity under the physical measure is approximately symmetric for large sized jumps, i.e. $LJV_{[t,t+\tau]}^P \approx RJV_{[t,t+\tau]}^P$. In the following simulation and empirical studies, we provide strong evidence for this conjecture and show that changes in the statistical jump measures play only a minor role in explaining the time variation in the tail risk premia. As a result, the difference between the two jump tail premia becomes

$$LJP_{t,\tau} - RJP_{t,\tau} \approx E_t^Q\left(RJV_{[t,t+\tau]}^Q\right) - E_t^Q\left(LJV_{[t,t+\tau]}^Q\right) \tag{6}$$

The measure $LJP_{t,\tau} - RJP_{t,\tau}$ mimics the component of investor fears proposed in Bollerslev and Todorov (2011b) and Bollerslev, Todorov, and Xu (2015), which is implicit in the gap between the estimated objective and risk-neutral jump tail variations implied by the S&P 500 index and therefore associated with investors' attitudes towards market risks. In contrast to Bollerslev and Todorov (2011b) and Bollerslev, Todorov, and Xu (2015) who consider the aggregate stock market, we concentrate on the dynamics underlying the VIX market. Since the VIX is called the "investor fear gauge", $LJP_{t,\tau} - RJP_{t,\tau}$ based on the VIX can therefore be interpreted as the "fear of fear" in the present study. As noted in Bollerslev, Todorov, and Xu (2015), $LJP_{t,\tau}$ and $RJP_{t,\tau}$ both contain components that reflect the compensation for time-varying jump intensity risk, or the premia attached to variation in the investment opportunity set. Hence, the difference between $LJP_{t,\tau}$ and $RJP_{t,\tau}$ will be largely purged of such risk and effectively be attributable to the special compensation demanded by investors for rare disaster events even when the investment opportunity set remains the same over time. In the rest of the paper, we employ $(LJP_{t,\tau} - RJP_{t,\tau})$

as a proxy for fear in the VIX market. The details on the estimation of the Q jump tail measures are presented in Appendix.

3 Simulation Study

This section presents a simulation study to examine the role of jump risk premium in affecting the time series properties of $VVIX^2_{[t,t+\tau]}$ and $VVRP_{t,\tau}$. We also extract the left and right jump tail variations and evaluate their contributions to the two risk measures considered.

3.1 Design

We first extend the jump-diffusion model for the pricing of VIX derivatives in Park (2016) by allowing for risk premia in both upward and downward jumps. The dynamics under the risk-neutral measure takes the following form

$$\begin{aligned} dv_t &= \kappa_v (u_t - v_t)\, dt + \sqrt{w_t} dB^Q_{1t} + J^Q_1 dN^Q_{1t} + J^Q_2 dN^Q_{2t} \\ &\quad -\lambda_+ \delta_+ dt - \lambda_- \delta_- dt \\ du_t &= \kappa_u (\overline{\mu} - u_t)\, dt + \sigma_u dB^Q_{2t} \\ dw_t &= \kappa_w (\overline{w} - w_t)\, dt + \sigma_w \sqrt{w_t} dB^Q_{3t} \end{aligned} \tag{7}$$

where $v_t = \log(VIX_t)$, u_t denotes the long-run mean of the VIX and w_t captures the variation in the volatility of the VIX. The processes B^Q_{1t}, B^Q_{2t} and B^Q_{3t} are standard Brownian motions, among which B^Q_{1t} and B^Q_{3t} are correlated with the coefficient ρ. In the VIX dynamics, we accommodate both upward and downward jumps driven by independent compound Poisson processes. They are characterized by N^Q_{1t} (N^Q_{2t}) that represents a risk-neutral Poisson process generating upward (downward) jumps with intensity λ_+ (λ_-). The size of upward (downward) jumps is denoted by J^Q_1 (J^Q_2), following an independent exponential distribution with a positive (negative) mean, i.e. $\delta_+ > 0$ ($\delta_- < 0$).

The corresponding system under the physical measure becomes

$$\begin{aligned} dv_t &= \kappa_v\left(u_t - v_t\right)dt + \sqrt{w_t}dB_{1t}^P + J_1^P dN_{1t}^P + J_2^P dN_{2t}^P \\ &\quad -\lambda_+^*\delta_+^* dt - \lambda_-^*\delta_-^* dt \\ du_t &= \kappa_u\left(\overline{\mu} - u_t\right)dt + \eta_u u_t dt + \sigma_u dB_{2t}^P \\ dw_t &= \kappa_w\left(\overline{w} - w_t\right)dt + \eta_w w_t dt + \sigma_w\sqrt{w_t}dB_{3t}^P \end{aligned} \tag{8}$$

where B_{1t}^P, B_{2t}^P and B_{3t}^P are standard Brownian motions, $\eta_u u_t$ and $\eta_w w_t$ drive the risk premia for the u_t and w_t processes. To introduce jump risk premia, we allow upward and downward jumps under the physical measure to have their own jump intensity and jump-size distributions specified by the parameters λ_+^*, δ_+^*, λ_-^* and δ_-^*. Similar to the simulation study conducted in Duan and Yeh (2010), we assume the means of jump sizes are the same under P and Q with $\delta_+^* = \delta_+$ and $\delta_-^* = \delta_-$, and allow for different jump intensities under the change of measure. As such, we define the upward and downward jump risk premia by $\phi_+ = \lambda_+ - \lambda_+^*$ and $\phi_- = \lambda_- - \lambda_-^*$, respectively[1]. The specification in equation (8) preserves the affine structure of the framework under different measures.

The simulation of VIX is generated using an Euler discretized version of (8) based on 78 intervals[2] for each of the $T = \tau \times 200$ trading day in the sample. A daily series is extracted by sampling once every 78 data points. The parameter values used are taken directly from those reported in the last column of Table 3 in Park (2016), with the parameter capturing the persistence of the volatility process k_w adjusted to ensure the positivity of the volatility in our simulation

[1] We also consider forcing an equality on jump intensities and allow the jump sizes to vary from the physical probability measure P to the risk-neutral pricing measure Q, in which case the jump risk premia is defined as $\phi_+ = \delta_+^* - \delta_+$ and $\phi_- = \delta_-^* - \delta_-$. Results on the contribution of jump tail variations to the $VVIX^2$ and $VVRP$ are qualitatively similar and therefore not reported for brevity.

[2] We assume 1 day consists of 6.5 hours of open trading and consider a sparse sampling at a frequency of once every 5 minutes. This results in 78 intraday intervals in a day, i.e. $\frac{6.5\times 3600}{300} = 78$.

experiment.

k_v	ρ	k_u	$\overline{\mu}$	σ_u	η_u	k_w
6.576	0.794	0.258	3.106	0.293	-0.024	1.8
$\overline{w}$	σ_w	η_w	λ_+	δ_+	λ_-	δ_-
1.956	1.976	-2.15	2.682	0.266	2.042	-0.217

The processes v_t, u_t and w_t are respectively initialized at 2, 2 and 0.2, which are given by the unconditional means of the corresponding series in our empirical study. We assume one year has 252 trading days.

We then compute the option prices of VIX corresponding to different strikes and maturities (τ) using the jump diffusion model under the risk-neutral probability measure in (7). To improve simulation accuracy, we rely on the empirical martingale simulation procedure introduced by Duan and Simonato (1998) and set the simulation path for option pricing to 10,000. Based on the simulated options on each trading day, we construct $VVIX^2_{[t,t+\tau]}$ with various maturities as in section 2 and compute the realized variance comprising the price information in the next τ days. Finally, we select both the implied and realized variances on the trading day that follows the previous maturity date so that we obtain non-overlapping samples with size equal to 200. All of our results reported below are based on a total of 1000 replications.

3.2 Results

Table 1 reports the mean values of $VVIX^2_{[t,t+\tau]}$ and $VVRP_{t,\tau}$ with 6 different maturities. To identify the impact of jump risk premia on the properties of the risk measures, we vary the magnitude of the upward (downward) jump premium ϕ_+ (ϕ_-) from 2 to 10 while restricting the downward (upward) jump premium ϕ_- (ϕ_+) to zero. The parentheses report the percentage changes of the mean values of $VVIX^2_{[t,t+\tau]}$ and $VVRP_{t,\tau}$ relative to their corresponding values in the case where there exist no jump risk premia, i.e. $\phi_+ = \phi_- = 0$. We show that for the same magnitude of jump risk premium, the upward jump premium generates a larger impact on $VVIX^2_{[t,t+\tau]}$ and $VVRP_{t,\tau}$ when compared to the downward jump premium. As maturity grows,

the two risk measures are generally less sensitive to the presence of jump premia.

Figure 1 is a heat map showing mean values of $VVIX^2_{[t,t+\tau]}$ and $VVRP_{t,\tau}$ over different combinations of the maturity and jump risk premia. We find that the term structure of $VVIX^2_{[t,t+\tau]}$ and $VVRP_{t,\tau}$ are highly responsive to upward jump premium ϕ_+, exhibiting a greater slope in magnitude as the jump premium grows. However, the downward jump premium ϕ_- delivers only trivial effects on the shape of the term structure with the slope virtually unaffected by the variation in ϕ_-. Our results in Figure 1 are generally consistent with the empirical findings in the existing literature and complement Christoffersen, Jacobs, and Ornthanalai (2012) for the important role of jump risk premium in the implied volatility term structure. In summary, our simulation reveals the dominant role played by the upward jump premium, indicating that the right jump tail risk premium associated with the large upward jumps may constitute the primary source of variation in $VVIX^2_{[t,t+\tau]}$ and $VVRP_{t,\tau}$.

In the simulation above, we only allow for the presence of one type of jump risk premium, i.e. upward or downward, to ascertain their different roles in affecting the dynamics of the risk measures. This obviously contradicts the real-life observations where the upward and downward jump premia often coexist. Going one step further, we simultaneously incorporate the two different jumps in the VIX dynamics and construct the right and left jump tails using the method discussed in section 2. Unlike the empirical study in which the VIX OTM puts are much less traded, our simulation study ensures that there are equal numbers of the OTM puts and calls, which alleviates the issue of measurement errors in the comparison of right and left jump tails.

Panel A of Table 2 reports the mean values of the jump tail variation under both P and Q measures[3]. In line with Bollerslev, Todorov, and Xu (2015) and Ellwanger (2017), we find that the P jump tail variation measures are dwarfed by the corresponding Q measures in the presence of the jump risk premia. Hence, we conclude that changes in the jump tail premia are primarily due to

[3]Details on the construction of the left and right jump tail variation measures under P from the return data can be found in Appendix.

movements in the tail variations under the Q measure. In addition, we investigate the hypothesis of symmetry of the jump tail risk under different probability measures. The last column in Panel A shows that the null hypothesis under the P measure is only rejected in 6% of the simulation repetitions whereas the rejection is obtained in almost all cases under the Q measure. Confirming Bollerslev, Todorov, and Li (2013), Bollerslev, Todorov, and Xu (2015) and Andersen, Todorov, and Ubukata (2021), the P jump process is approximately symmetric deep in the tails. In contrast, the Q expectation of the right jump tail variation exceeds its left counterpart in magnitude.

To assess the contribution of the Q jump tail variation measures to $VVIX^2_{[t,t+\tau]}$ and $VVRP_{t,\tau}$, we run the following regression with a focus on the monthly horizon

$$y_{j,t} = \alpha_{ij} + \beta_{ij} x_{i,t} + \varepsilon_{ij,t} \tag{9}$$

where $y_{j,t}$ denotes the measure j among a set of J candidates, $j = 1, \cdots, 6$, namely $VVRP_{t,30}$, $VVRP_{t,180}$ the $VVRP$ slope defined as the ($VVRP_{t,180}$−$VVRP_{t,30}$) as well as the three corresponding measures for the $VVIX^2$; the jump tail variation is given by $x_{i,t}$ with $x_{1,t}$ denoting the right tail and $x_{2,t}$ representing the left tail. To account for the issue of serial correlation, we derive the statistical significance using Newey and West (1987) robust t-statistics with an optimal lag. Panel B of Table 2 reports the mean values of the adjusted R^2 for the regressions based on the $VVRP$ with the proportion of significant results indicated in the parentheses. We find that the right jump tail outperforms the left jump tail in explaining the dynamics underlying $VVRP_{t,30}$ and the $VVRP$ slope while the evidence is weak for the long-term $VVRP$. The corresponding results for the $VVIX^2$ are provided in Panel C. Although the two tails both contribute significantly to variations in the short- and long-term $VVIX^2$ as well as its term structure, the right tail demonstrates a much higher degree of explanatory power. Our results in Table 2 therefore confirm the findings in Table 1 that the upward jump premium plays a dominant role in affecting the properties of $VVIX^2_{[t,t+\tau]}$ and $VVRP_{t,\tau}$.

Recall equation (6) for the proxy of the fear-of-fear factor

$$LJP_{t,\tau} - RJP_{t,\tau} \approx E_t^Q \left(RJV^Q_{[t,t+\tau]} \right) - E_t^Q \left(LJV^Q_{[t,t+\tau]} \right)$$

With equal numbers of OTM calls and puts, our simulation clearly points towards the superiority of $RJV^Q_{[t,t+\tau]}$ over its left counterpart not only in terms of the magnitude but also on the contribution to the relevant risk measures. In practice, OTM VIX calls are often considered a form of tail risk hedges. This can be explained by the leverage effect that negative variations in returns are closely associated with rises in volatility, in which case OTM VIX calls can hedge. As a result, OTM call options are more heavily traded in the real VIX market, suggesting that the size of $RJV^Q_{[t,t+\tau]}$ may further exceed that of $LJV^Q_{[t,t+\tau]}$ in the empirical study. Hence, we obtain the following approximation given by

$$LJP_{t,\tau} - RJP_{t,\tau} \approx E_t^Q \left(RJV^Q_{]t,t+\tau]} \right) \tag{10}$$

Since the right jump tail is a key contributor to the level and slope of $VVIX^2_{[t,t+\tau]}$ and $VVRP_{t,\tau}$, it may also perform as the primary component providing return predictive power for these measures, which we verify below in our empirical study. For ease of notation, we abbreviate $VVIX^2_{[t,t+\tau]}$, $VVRP_{t,\tau}$ and $RJV^Q_{[t,t+\tau]}$ by $VVIX^2_t$, $VVRP_t$ and RJV^Q_t, respectively, when $\tau = 30$ is considered in the rest of the paper.

4 Data

VIX futures data are collected from the $CBOE$ website and span from March 26, 2004 through December 31, 2020. On each trading day during the sample period, three to six different maturities are traded. We rely on the daily settlement prices to obtain the realized variance of VIX. In addition, the raw VIX options data originate from OptionMetrics covering the period of February 24, 2006 to December 31, 2020. As a result, our sample is restricted to the shorter period when

examining the joint information content from the data of futures and options. For robustness, we also consider an alternative measure of statistical volatility-of-volatility based on the 5-minute VIX futures returns. The data is sourced from Tick Data Inc. and starts in July 2012.

We apply standard filters to the raw options data to eliminate inaccurate or illiquid options. First, we delete the VIX options for which the price, defined as the midpoint of the option bid and ask quotes, is less than 0.2 or the trading volume is zero. Second, options with Black-Scholes implied volatility (BSIV) lower than 10% or greater than 150% are excluded from the sample. Third, we focus on options with 8 to 90 days to expiration. This leaves us with more than a million VIX option quotes, with a daily average of 102.7 VIX OTM calls and 41.3 puts over the full sample. The number of VIX OTM options on a given date increases with time, with around 25.9 calls (11.2 puts) at the beginning of the data set and around 136.5 calls (87.9 puts) at the end. To assess whether the return predictability (previously ascribed to the popular risk measures) is effectively arising from the right jump tail, we follow Bollerslev, Todorov, and Xu (2015) in constructing the jump tails using OTM options with maturities between 8 and 49 calendar days. It is worth noting that all of our risk measures are non-overlapping. Taking the monthly horizon as an example, the implied variance measures are given by the values at the end of the month and the realized variance is derived over the following month and annualized.

In addition to the risk measures introduced in section 2, we also consider a variety of predictor variables that are widely employed in the existing literature of return predictions (see, for instance, Neely et al. (2014), Park (2015) and Cakmakli and van Dijk (2016)). Data on the P/E ratio and dividend yields are taken from Standard & Poor's. The default spread (the difference between Moody's BAA and AAA corporate yields), the term spread (the difference between the 10-year and 3-month Treasury yields) and the TED spreads are all sourced from the website of the Federal Reserve Bank of St. Louis. We also consider the Economic Policy Uncertainty (EPU) index of Baker, Bloom, and Davis (2016) and the risk aversion index of Bekaert, Engstrom, and Xu (2022).

Both are downloaded from the authors' websites[4].

5 Empirical Results

5.1 Preliminary data analysis

As option returns are heavily influenced by shocks in the underlying asset price and volatility, we employ the approach of Bakshi and Kapadia (2003) and Huang et al. (2019) to derive the delta-hedged option gains that are unaffected by the underlying asset's price risk:

$$\pi_{t,t+\tau} = C_{t+\tau} - C_t - \sum_{n=0}^{N-1} \Delta_{t_n}(F_{t_{n+1}} - F_{t_n}) - \sum_{n=0}^{N-1} r_f C_t \frac{\tau}{N} \tag{11}$$

where $t_0 = t$, $t_N = t + \tau$ refers to the maturity date, and Δ_{t_n} indicates the option delta that is available from OptionMetrics. We then scale the delta-hedged option gain by the initial option price $\pi_{t,t+\tau}/C_t$ and take an average of the gains over their respective moneyness and maturity category. Specifically, we separate OTM options by call or put and classify each option into 2 bins by moneyness that is defined as $k = K/F_t(\tau)$. Following Bakshi and Kapadia (2003), we consider a sample of options with constant maturity, i.e. 30 and 60 days, to avoid overlapping observations of option returns. To obtain the returns on VIX futures, we make use of the front contracts and roll over to the next maturity contract in the case where the shortest contract has less than 5 days to maturity, see also in Taylor (2019).

Panel A of Table 3 reports the descriptive statistics of the delta-hedged option returns across different moneyness bins and maturity. Overall, OTM delta-hedged VIX options have significantly negative returns and the delta-hedged gains become more negative when the hedging horizon is extended from 30 days to 60 days. In addition, option returns exhibit mild serial correlation, which are dealt with in the subsequent predictive regressions. Panel B of Table 3 presents the results of VIX futures returns. Similar to returns of S&P 500, VIX returns are approximately serially

[4]The time series of EPU index is obtained from http://www.policyuncertainty.com and that of the risk aversion index is from https://www.nancyxu.net/risk-aversion-index.

uncorrelated, with a mean indistinguishable from zero. All the findings above are consistent with those reported in previous studies.

Summary statistics for the monthly predictor variables are reported in Table 4. In constructing $VVRP_t$, defined as the difference between $E_t^P\left(QV_{[t,t+\tau]}\right)$ and $E_t^Q\left(QV_{[t,t+\tau]}\right)$, for forecasting purpose, we rely on the HAR model of Corsi (2009) to obtain a direct forecast for $RVVIX_{[t,t+\tau]}$ that can be approximated as $E_t^P\left(QV_{[t,t+\tau]}\right)$. Inspired by Li and Zinna (2018) who point out the significance of the variance risk premium term structure for stock return predictability, we also consider the slope of $VVRP_t$ defined as $VVRPS_t = VVRP_{t,90} - VVRP_t$. The slope of $VVIX_t^2$ is therefore computed as $VVIXS_t = VVIX_{[t,t+90]}^2 - VVIX_t^2$. To isolate the effects of the right jump tail variation, we obtain the components of the $VVIX_t^2$ and $VVRP_t$ striped of RJV_t^Q, $VVIX_t^2 - RJV_t^Q$ and $VVRP_t - RJV_t^Q$, denoted as $VVIX_t^{2n}$ and $VVRP_t^n$.

To examine whether the predictive power afforded by $VVRP_t$, $VVIX_t^2$ and RJV_t^Q is robust to other pricing factors, we include the following control variables in our regressions and classify them into six distinct groups: 1) macroeconomic variables including log price-earnings ratio (P_t/E_t), log price-dividend ratio (P_t/D_t), the default spread $(DFSP_t)$ and the term spread $(TMSP_t)$; 2) technical indicators introduced by Neely et al. (2014), among which we select the moving-average indicator (MA_t) and the momentum indicator (MOM_t)[5]; 3) uncertainty measures including the U.S. EPU index (EPU_t) of Baker, Bloom, and Davis (2016) and the risk aversion index (RA_t) of Bekaert, Engstrom, and Xu (2022); 4) limits of arbitrage proxied by the TED spreads (TED_t); 5) option market liquidity as measured by the relative bid-ask spreads $(SPREAD_t)$ of the VIX options; 6) jump fears captured by the option-implied skewness $(SKEW_t)$ in the work of Bakshi, Kapadia, and Madan (2003)[6]. Groups 1), 2) and 3) are considered in the predictions of VIX futures returns and groups 3), 4), 5) and 6) for the case of option returns. Given the existing literature, there is no surprise that many of the traditional predictor variables,

[5] In constructing MA_t, we let the length of the short MA (s) be 2 and the length of the long MA (l) be 9; we consider $m = 12$ for the momentum indicator, see more details in Neely et al. (2014).

[6] More details on the calculation of $SKEW_t$ using the VIX options data can be found in Appendix.

e.g. macroeconomic variables and uncertainty measures in particular, exhibit strong persistence with first-order autocorrelations in the range of 0.80 and 0.98. In a sharp contrast, $VVIX_t^2$ and $VVRP_t$ are substantially less persistent, thereby balancing the regression for returns in terms of the integration order and generating fewer econometric problems.

In light of the correlation matrix reported in the lower panel of Table 4, we conjecture that, compared with the risk aversion index RA_t, the fear-of-fear proxied by RJV_t^Q may capture distinct investor proclivities. Specifically, while RA_t is negatively correlated with RJV_t^Q, it displays positive relationships with both $VVIX_t^2$ and $VVIX_t^{2n}$. This implies that RA_t may reflect investors' attitudes towards the temporal variation in volatility-of-volatility or continuous price moves in the VIX market rather than the fear for jump tail events. As a different measure of uncertainty in the present study, EPU_t positively correlates with our fear proxy but the correlation is relatively small at 0.157. Intuitively, high values of EPU_t result in increased market fear through investor sentiment when economic policies are difficult to anticipate. Consistent with the finding by Bekaert, Engstrom, and Xu (2022), RA_t displays a correlation of 0.342 with EPU_t. However, their opposite relationships with RJV_t^Q suggest that they may measure uncertainty via different mechanisms.

We also report in Figure 2 the time series plots of the main risk measures introduced in section 2 along with the two uncertainty measures. That VIX options only started in 2006, and that the deep OTM options were infrequently traded in early stage, explains missing values in the series of RJV_t^Q. A few differences between the series of $VVIX_t^2$ and RJV_t^Q are noted. For example, $VVIX_t^2$ reaches high values during the 2008 financial crisis and 2010 flash crash before attaining its maximum around early 2020 when the pandemic starts to heavily impact the global financial markets. Although RJV^Q grows steadily over the period of 2008 and 2010, it peaks around 2011-2012, coinciding with the European debt crisis. During the pandemic period, RJV_t^Q experiences an abrupt increase in Feb 2020, exhibiting a good coherence with $VVIX_t^2$. Notably, we document clearly different dynamics in the series of RA_t and EPU_t and the latter displays

more similar movements to RJV_t^Q, which corroborates the findings on the correlations discussed above. Moreover, RA_t, EPU_t and our fear proxy all rise sharply in early 2020 where the pandemic triggered a massive spike in uncertainty.

5.2 In-sample analysis

5.2.1 VIX futures returns

We start by assessing the role of right jump tail component in the in-sample predictions for the VIX futures returns given by

$$\frac{1}{h}\sum_{n=1}^{h} r_{t+n} = \beta_{0i}(h) + \beta_{1i}(h)x_{i,t} + \varepsilon_{i,t+h} \tag{12}$$

where r_t is the monthly VIX futures return and $x_{i,t}$ denotes the predictor i among various candidate predictors. As highlighted in section 5.1, several predictor variables, macroeconomic variables in particular, are highly persistent with autoregressive roots close to unity. This raises a common concern regarding the use of strongly persistent variables and the possibility of unbalanced regressions, which undermine the reliability of predictability tests (see more discussions in Campbell and Yogo (2006), Magdalinos and Phillips (2009) and Yang et al. (2020)). To address this problem, we employ the IVX approach of Kostakis, Magdalinos, and Stamatogiannis (2015) that exploits instrumental variables with a lower degree of persistence than that of the predictive variables. The method is not only robust to the time-series properties of the predictors, covering the entire range from stationarity to pure nonstationarity of unit root series, but also eliminates the endogeneity issue.

Table 5a reports the results from the monthly return regressions using the IVX estimator and the corresponding Wald statistics under the null of no predictability. For ease of interpretation, in dividing each explanatory variable by its standard deviation, the estimated coefficient represents the effect of a one standard deviation change in that variable. Unless otherwise stated, in what follows, we always preprocess the data in such a manner when conducting estimations. In addition,

all coefficient estimates are scaled up by a factor of 100 for presentation purposes. The univariate regressions on the left panel of Table 5a show that $VVRP_t$ dominates $VVIX_t^2$ and all the other traditional predictors in terms of the sample fit[7]. Combining $VVRP_t$ with other predictors only leads to a marginal increase in the (adjusted) R^2. Notably, several predictors, e.g. the default spread ($DFSP_t$), the moving-average indicator (MA_t) and EPU_t, that exhibits the evidence of predictability in the univariate regression are no longer significant in the multiple regression with $VVRP_t$. A similar observation on the superiority of $VVRP_t$ is also established for the quarterly return regressions in Table 5b. For annual regressions reported in Table 5c, P_t/D_t, the default spread ($DFSP_t$), the term spread ($TMSP_t$) and the two uncertainty measures show a higher degree of return predictability than $VVRP_t$. This is largely in line with many of the empirical studies which show that the predictive power of the traditional predictors tends to be the strongest over longer multi-year horizons. Finally, it is worth noting that, regardless of the time horizon and the inclusion of other traditional predictive variables, $VVRP_t$ remains statistically significant at the 1% level or better.

To identify the source of the predictive power afforded by $VVRP_t$, we decompose $VVRP_t$ into the diffusive and jump tail risk components and run the predictive regressions based on these different components together with the control variables for monthly, quarterly and annual returns. The results are summarized in Tables 6a to 6c, respectively. Similar to the construction of $VVRP_t^n$, the slope of $VVRP_t$ deprived of the right jump tail variation is derived as $VVRPS_t^n = \left(VVRP_{t,90} - RJV^Q_{[t,t+90]}\right) - \left(VVRP_t - RJV_t^Q\right)$ with $RJV^Q_{[t,t+90]}$ obtained by averaging the daily measures within 90 days. We show that, for various time horizons, subtracting RJV_t^Q from $VVRP_t$ results in less significant Wald−statistics and little return predictability underlying $VVRP_t^n$. We

[7] In Kostakis, Magdalinos, and Stamatogiannis (2015), the IVX instruments are constructed by suitably filtering the actual predictor and the coefficient estimates of the predictive regression are obtained by employing a two-stage least-squares estimator. The adjusted R^2 reported in the present paper is based on the residual vector from the second stage of the two-stage least squares procedure, namely the prediction errors, and therefore is considered an appropriate measure for model comparison. Our calculation of the adjusted R^2 is in the spirit of Pesaran and Smith (1994) who propose the generalized R^2 in the context of instrumental variable regressions.

also find that the term structure $VVRPS_t$ is nontrivial in return predictions but an evident increase in the R^2 driven by $VVRPS_t$ is only obtained at annual horizons. Similar to the univariate case where only $VVRP_t$ is considered, the removal of RJV_t^Q from $VVRP_t$ and $VVRPS_t$ substantially reduces the R^2 and renders the Wald−statistics for $VVRP_t^n$ and $VVRPS_t^n$ less significant. In addition, adding RJV_t^Q to the regression based on $VVRP^n$ and $VVRPS^n$ increases the R^2 where the values exceed those implied by $VVRP_t$ and $VVRPS_t$ over monthly and quarterly horizons.

Finally, we include other traditional predictors in the regressions based on $VVRP_t^n$, $VVRPS_t^n$ and RJV_t^Q and provide evidence for the significance of $VVRP_t^n$ and RJV_t^Q in all the cases considered. We therefore conclude that much of the return predictability afforded by $VVRP_t$ is attributable to the right jump tail variation and that the predictability results are robust to various control variables.

5.2.2 VIX options returns

To ascertain the role of right jump tail variation in pricing the delta-hedged option gains, we follow Bakshi and Kapadia (2003) and Huang et al. (2019) in constructing the following regression based on the fixed option maturity

$$GAINS_{t,t+\tau} = \frac{\pi_{t,t+\tau}}{C_t} = \theta_{0i} + \theta_{1i} x_{i,t} + \gamma_i GAINS_{t-\tau} + \varepsilon_{i,t+\tau} \tag{13}$$

Delta-hedged option returns $GAINS_{t,t+\tau}$ realized over 30 and 60 days are regressed from expiration to expiration on the value of $x_{i,t}$ at the end of the previous expiration. As mentioned in section 5.1, option returns display some degree of autocorrelation and thus may alleviate the concern related to the use of unbalanced regressions that has been extensively investigated in the literature of market return predictions. Given this, we follow the mainstream literature on option return predictions by including the lagged gains in equation (13) to correct for the serial correlation present in the residuals. The null of no predictability by each of the predictor variables is examined by the Newey-West procedure with an optimal lag.

Tables 7a and 7b report the predictive regression results for OTM call option returns over 30 and 60 days, respectively[8]. The Box-Pierce test with 6 lags (Q_6) is undertaken to detect the level of residual autocorrelation. The results show that $VVIX_t^2$ significantly predicts the future option returns with a negative sign and a reasonable fit similar to that reported in Bakshi and Kapadia (2003). In contrast, the predictions by $VVRP_t$ are only marginally significant for 30-day options and insignificant for 60-day options. The superiority of $VVIX_t^2$ over $VVRP_t$ in predicting the VIX option returns is also reported in the work of Park (2015). In the univariate regressions, none of the other predictors exhibits predictive ability with the exception of TED_t and $SPREAD_t$ that are significant at 10% level for 30-day options. Combined with the traditional predictors for option returns, $VVIX_t^2$ retains its significance across different moneyness levels and time horizons, suggesting that none of the other predictors have incremental predictive power beyond $VVIX_t^2$.

To further examine the role of RJV_t^Q in the option return predictability afforded by $VVIX_t^2$, we adopt a similar decomposition procedure to that applied in the case of $VVRP_t$ for predicting VIX futures returns and report the results in Tables 8a and 8b. First, we show that the $VVIX_t^2$ term structure $VVIXS_t$ is trivial in enhancing the predictions based on $VVIX_t^2$ alone. Second, removing RJV_t^Q from $VVIX_t^2$ and $VVIXS_t$ leads to a 30%−40% reduction in the R^2 for 30-day option returns but produces little effect on the longer-dated options. Third, adding RJV_t^Q to the multiple regressions based on $VVIX_t^{2n}$ and $VVIXS_t^n$ increases the R^2 where the values are similar to those generated by $VVIX_t^2$ and its term structure. Across all the different cases, $VVIX_t^{2n}$ and RJV_t^Q remain significant even after other traditional predictor variables are controlled for. Our results suggest that, while RJV_t^Q helps explain a modest proportion of the losses incurred on the short-dated delta-hedged portfolios, $VVIX_t^2$ is the predominant measure providing significant forecasting power for VIX option returns.

[8]We focus on the OTM VIX calls since they are considered an important form of tail risk hedges (see Park (2015) for example) and therefore receive more attention from investors. Results for the OTM puts support our general conclusion on the predictability of option returns and are available upon request.

5.2.3 Robustness

Our investigation of the robustness of our predictability results uses alternative measures of volatility-of-volatility. For the risk-neural expectation of the volatility-of-volatility, we make use of the $VVIX$ index as well as its term structure from the $CBOE$. The index has been published since 2012 and back-filled to 2006. For the physical expectation, we rely on the 5-minute front-month VIX futures returns to compute $RVVIX_t$. Due to the availability of tick data, our analysis based on $RVVIX_t$ is from 2012 to 2020. In line with the previous analysis, all the variation measures are at a monthly frequency. Figure 3 depicts the time series plots of the $CBOE$ $VVIX$ index and our measure of $VVIX_t^2$ calculated using OTM options. Overall, the calculated $VVIX_t^2$ qualitatively match the evolution of the reported $VVIX$ index with a correlation coefficient of 95%. That our measure of $VVIX_t^2$ is on average lower than the $CBOE$ $VVIX$ may be attributable to two points. First, we obtain a broader strike range by including most of the option quotes that meet the conditions specified in section 4 and consider the interpolation and extrapolation procedure to approximate the integral on the RHS of equation (1). However, the $CBOE$ adopts a particular cutoff rule which may induce distortions, see Jiang and Tian (2005) and Andersen, Bondarenko, and Gonzalez-Perez (2015) for details. Second, our $VVIX_t^2$ is obtained using the options from the Optionmetrics database containing the last daily bid-ask quotes only, which might not perfectly match the data published by the $CBOE$ for their final end-of-day computation.

Next, we follow Bollerslev and Todorov (2011a) and Bollerslev, Todorov, and Li (2013) in using the high-frequency data to derive the continuous variation along with the realized jump tail variation under the statistical measure. The time series plots in Figure 4 show that the estimate for the left tail appears larger than the right, which is in parallel to the results reported in Bollerslev, Todorov, and Li (2013). We further confirm that the realized jump tail is approximately symmetric with the null hypothesis $LJV^P_{[t,t+\tau]} = RJV^P_{[t,t+\tau]}$ not rejected at the 5% level.

Finally, we estimate the predictive regressions over horizons ranging from 1 to 12 months using

new measures of the volatility-of-volatility risk and report the values of adjusted R^2 for VIX futures returns in Figure 5[9]. Consistent with the earlier empirical results, $VVRP_t$ outperforms the $CBOE\ VVIX$ over most of the horizons and the right jump tail is still the primary source of the forecasting power afforded by $VVRP_t$. Further to this, note that the greatest magnitude of return predictability is observed for the case where the right jump tail and the diffusive components are separately accommodated.

5.3 Out-of-Sample Analysis

Our in-sample results so far suggest that the right jump tail is a key driver of the predictability ascribed to $VVRP_t$ for VIX futures returns. In this subsection, we further evaluate the role of the right jump tail in the out-of-sample (OOS) forecasting exercises. Using a rolling window scheme, we employ half of the full sample for in-sample estimation and the remaining for performance evaluation.

We consider the out-of-sample R-squared (OOR^2) to measure the proportional decrease in the mean squared prediction error (MSPE) of the competition model relative to the historical average. A positive value of OOR^2 implies that the model of interest beats the historical average forecast in terms of the MSPE and a negative value indicates the opposite. We provide the OOS results in Table 9 where the highest values of OOR^2 in each of the two panels are indicated in bold. To examine the null that the MSPE of the historical average forecast is no greater than that of the predictive regression, we employ the Clark and West (2007) MSPE-adjusted statistics and report the results in Panel A. We find that the the MSPE-adjusted statistics given by $VVRP_t$ are significant in 10 out of 12 forecasting horizons, suggesting that $VVRP_t$ generally outperforms the historical average benchmark in the OOS forecasting practice. Note that the results of the

[9]Regression results on the return predictability of VIX futures are not reported but they are available upon request. The use of non-overlapping option returns further reduces the size of our sample based on the $CBOE\ VVIX^2$ and the high-frequency data of VIX futures. We therefore do not perform the predictive regressions for delta-hedged option returns due to the lack of observations.

MSPE-adjusted test are significant for a few cases associated with the negative values of OOR^2. A similar observation is documented in Neely et al. (2014). This arises from the fact that the adjusted MSPE test accounts for the upward bias in the MSPE of the alternative model with additional parameters that are zero under the null, see more discussions on the nested model forecasts in Clark and West (2007). When RJV_t^Q is removed from $VVRP_t$ in model 2, a reduction in the OOR^2 is observed across all the forecasting horizons and none of the predictions are significant. Finally, the reintroduction of RJV_t^Q in model 3 substantially increases the OOR^2 especially over short horizons and renders the MSPEs over different horizons significantly lower than those of the historical average.

Going one step further, we include other traditional predictor variables to model 3 based on $VVRP_t^n$ and RJV_t^Q and report the results in Panel B. The MSPE-adjusted statistic is computed to test the null that the MSPE generated by model 3 is less than or equal to the MSPE given by the various competition model in Panel B. We show that our benchmark model 3 is only outperformed by the inclusion of macroeconomic variables or uncertainty measures over 6-12 months. Adding technical indicators brings few significant gains beyond model 3 with the exception of predictions over 9- and 11-month horizon. Hence, our OOS results clearly point towards the superior role of RJV_t^Q in predicting VIX futures returns over short horizons.

As a final exercise, we evaluate the economic significance of the OOS forecasts by forming a trading strategy based on VIX futures and risk-free assets. Following Neely et al. (2014) and Pyun (2019), among others, we calculate the certainty equivalent return (CER) gain for a mean-variance investor who allocates across VIX futures and risk-free bills using forecasts of VIX futures returns. At the end of period t, the investor assigns the optimal weight to the VIX futures during period $t+1$

$$\omega_t = \frac{1}{\gamma}\frac{\widehat{r}^*_{t+1}}{\widehat{\sigma}^2_{t+1}} \tag{14}$$

where $\gamma = 3$ is assumed as the risk-aversion coefficient, $\widehat{r}^*_{t+1}$ denotes the forecast of VIX futures

excess returns, and the forecast-based realized variance of the VIX futures returns is used as a proxy for $\widehat{\sigma}^2_{t+1}$. We allow the investor to rebalance the portfolio weight at the same frequency as the forecasting horizon and restrict the portfolio weight to lie between $[-0.5, 1.5]$ for the consideration of short sales. The period$-t+1$ portfolio return is therefore

$$R_{p,t+1} = \omega_t r^*_{t+1} + rf_{t+1} \tag{15}$$

where r^*_{t+1} is the VIX futures excess returns and rf_{t+1} is the risk-free rate[10]. The CER is obtained as

$$CER = \overline{R_p} - \frac{\gamma}{2}\widehat{Var}(R_p) \tag{16}$$

where $\overline{R_p}$ and $\widehat{Var}(R_p)$ denote the sample mean and variance of the portfolio returns, respectively.

In Panel A of Table 9, the CER gain is derived as the difference between the CER of the forecasts generated by models 1, 2 and 3 and the CER of the historical average forecast. In Panel B, we compare the CER of various competition models, i.e. models 4, 5 and 6, with that given by model 3. As suggested in Campbell and Thompson (2008) and Rapach, Strauss, and Zhou (2010), the CER gain can be interpreted as the portfolio management fees that investors are willing to pay to utilize the information in the predictive regression forecast in place of the forecast delivered by the benchmark model. Panel A shows that the investment strategy based on $VVRP_t$ results in positive CER gains over various horizons where gains are considerably diminished when RJV_t^Q is subtracted from $VVRP_t$ in model 2. The highest CER gains are attained by the predictive regression including RJV_t^Q in model 3 except for 7-month to 10-month horizons, suggesting that the information contained in RJV_t^Q has substantial economic value for a risk-averse investor, especially over short horizons. Considering other traditional predictors in Panel B, we show that, although the CER gains can be further enhanced over longer horizons, model 3 still dominates the alternatives, at least over monthly horizon.

[10]The three-month T-bill data (risk-free rate) is obtained from the public website of the Federal Reserve Bank of St. Louis.

6 Conclusion

The paper examines the role of fear-of-fear in determining the properties of the variance-of-variance risk premium ($VVRP_t$) and volatility-of-volatility ($VVIX_t^2$) as well as their predictive power for returns in the VIX market. We adopt the difference between the upward and downward jump risk premia associated with sizeable price moves as a proxy for the fear-of-fear, since it reflects the the compensation for rare jump events and is largely independent of the temporal variation in asset prices. Our simulation shows that the risk-neutral right jump tail variation (RJV_t^Q) dominates the left tail as a key driver of $VVRP_t$ and $VVIX_t^2$. With plausible assumptions, we conjecture that the fear component embedded in the VIX market can be approximated by RJV_t^Q.

Our empirical study is based on the VIX options and futures from 2006 to 2020. We present novel in-sample evidence for the superior performance of $VVRP_t$ in the return predictions of VIX futures and the dominant role of RJV_t^Q in providing the strong predictive power underlying $VVRP_t$. An out-of-sample forecasting exercise shows that RJV_t^Q not only accounts for much of the return predictability afforded by $VVRP_t$ but also generates nontrivial economic value, especially over short horizons. In particular, from 1-month to 5-month horizon, the predictive regression based on the diffusive component of $VVRP_t$ and RJV_t^Q serves as the top performer even against other traditional predictor variables. With the delta-hedged option returns, we find that, while RJV_t^Q plays an important role for short-dated options, $VVIX^2$ is the primary source of the negative gains of delta-hedged portfolios.

The present paper concentrates on using jump tail variation to capture investor fears implicit in the VIX market. Although we include the Risk Aversion index and the Economic Policy Uncertainty index as control variables in our predictive regressions, further research might investigate how our jump tail risk measures differ from market-based sentiment indicators. This could deliver a deeper understanding of differences in risk attitudes in the VIX market and in the aggregate stock market. It might also be rewarding to examine whether the fear proxied by the jump tail

variation could be used to forecast rare disasters relevant to the VIX market or future returns of the aggregate market. Moreover, incorporating the jump tail risk analyzed here might further improve the VIX derivatives pricing and reveal important dynamics of S&P 500 returns.

7 Appendix

7.1 Jump Tail Variation Under the Risk-Neutral Measure

Our estimation of the Q jump tail measures follows Bollerslev, Todorov, and Xu (2015). Assuming that the tail parameters remain constant over the maturity τ, the left and right jump tail variations can be written as

$$\begin{aligned} LJV^{Q}_{[t,t+\tau]} &= \tau\phi_t^{-}e^{-\alpha_t^{-}|k_t|}\left(\alpha_t^{-}k_t\left(\alpha_t^{-}k_t+2\right)+2\right)/\left(\alpha_t^{-}\right)^3 \\ RJV^{Q}_{[t,t+\tau]} &= \tau\phi_t^{+}e^{-\alpha_t^{+}|k_t|}\left(\alpha_t^{+}k_t\left(\alpha_t^{+}k_t+2\right)+2\right)/\left(\alpha_t^{+}\right)^3 \end{aligned} \tag{17}$$

where the level shift parameters $\phi_t^{\pm}$ and the shape parameters $\alpha_t^{\pm}$ are allowed to vary independently over time, and the threshold k_t defines large jumps. The estimation of $\phi_t^{\pm}$ and $\alpha_t^{\pm}$ are based on the close-to-maturity and deep OTM puts and calls for the left and right tails, respectively. The intuition is that such options may more effectively isolate jump tail risk since they are worthless unless jumps occur in the underlying asset.

Let $O_{t,\tau}(k)$ represent the time t price of an OTM option with time to maturity τ and log-moneyness k. It follows from Bollerslev and Todorov (2011b) that the ratio of two OTM options with the same maturity τ but different strikes does not rely on $\phi_t^{\pm}$, giving rise to the estimator proposed by Bollerslev and Todorov (2014)

$$\widehat{\alpha}_t^{\pm} = \arg\min_{\alpha^{\pm}} \frac{1}{N_t^{\pm}}\sum_{i=1}^{N_t^{\pm}}\left|\log\left(\frac{O_{t,\tau}(k_{t,i})}{O_{t,\tau}(k_{t,i-1})}\right)(k_{t,i}-k_{t,i-1})^{-1}-\left(1\pm\left(-\alpha^{\pm}\right)\right)\right| \tag{18}$$

where $N_t^{\pm}$ demotes the total number of options used in the estimation with $0 < |k_{t,1}| < \cdots <$

$\left|k_{t,N_t^{\pm}}\right|$. Based on a given $\alpha^{\pm}$, the level shift parameters can be estimated by

$$\widehat{\phi}_t^{\pm} = \arg\min_{\phi^{\pm}} \frac{1}{N_t^{\pm}} \sum_{i=1}^{N_t^{\pm}} \left| \log\left(\frac{e^{r_{t,\tau}} O_{t,\tau}(k_{t,i})}{\tau F_{t-,\tau}}\right) - (1 \mp \widehat{\alpha}_t^{\pm}) k_{t,i} + \log\left(\widehat{\alpha}_t^{\pm} \mp 1\right) + \log(\widehat{\alpha}_t^{\pm}) - \log(\phi^{\pm}) \right| \tag{19}$$

where $r_{t,\tau}$ denotes the risk-free interest rate over the $[t,\, t+\tau]$ time interval, and $F_{t,\tau}$ represents the time t futures price of $VIX_{t+\tau}$. In practice, we employ OTM VIX call options with log-moneyness greater than 1.5 times the normalized at-the-money (ATM) BSIV and set the cutoff k_t equal to 2.5 times the normalized ATM BSIV at time t[11]. Furthermore, we allow α_t^+ and ϕ_t^+ to vary on a daily basis and the monthly jump tail variation is constructed by averaging the daily measures within the month.

7.2 Jump Tail Variation Under the Physical Measure

This section provides details on the estimation of P jump tails from high-frequency VIX futures data following the work of Bollerslev and Todorov (2011a) and Bollerslev, Todorov, and Li (2013). Let the discrete time grid be $0,\, \frac{1}{n},\, \frac{2}{n}, \cdots,\, T$ where n denotes the sampling frequency and T the time span, we express the log-price increments over the time interval $[\frac{i-1}{n},\, \frac{i}{n}]$ by $\Delta_i^n p = p_{\frac{i}{n}} - p_{\frac{i-1}{n}}$. We first derive the realized variation and bi-power variation given by

$$\begin{aligned} RV_t &= \sum_{i=tn+1}^{tn+n} |\Delta_i^n p|^2 \\ BV_t &= \frac{\pi}{2} \sum_{i=tn+2}^{tn+n} |\Delta_i^n p| \left|\Delta_{i-1}^n p\right| \end{aligned} \tag{20}$$

With $n \to \infty$, the bi-power variation consistently estimates only the component of the total variation associated with continuous price movements.

[11] We also consider other choices for the thresholds and the results of the return predictability are qualitatively similar.

Next, we compute the Time-of-Day (TOD) factor as given by

$$TOD_i = \frac{n\sum_{t=1}^{T}\left|\Delta_{i_t}^n p\right|^2 1\left(\left|\Delta_{i_t}^n p\right| \leq \eta\sqrt{BV_t \wedge RV_t}n^{-\varpi}\right)}{\sum_{s=1}^{nT}\left|\Delta_s^n p\right|^2 1\left(\left|\Delta_s^n p\right| \leq \eta\sqrt{BV_{[s/n]} \wedge RV_{[s/n]}}n^{-\varpi}\right)} \tag{21}$$

where $i_t = (t-1)n + i$, $i = 1, \cdots, n$, $\eta > 0$ and ϖ are both constants. In line with Bollerslev, Todorov, and Li (2013), we set $\eta = 2.5$ and $\varpi = 0.49$, indicating that we classify all of the high-frequency price moves that exceed 2.5 standard deviations of a local estimator of the corresponding stochastic volatility as jumps. We then estimate the continuous variation as follows

$$CV_t = \sum_{i=tn+1}^{tn+n}\left|\Delta_i^n p\right|^2 1\left(\left|\Delta_i^n p\right| \leq \alpha_i n^{-\varpi}\right) \tag{22}$$

To isolate the realized jumps from the continuous price movements, we calculate the truncation parameter as

$$\alpha_i = \eta\sqrt{BV_{[i/n]} \wedge RV_{[i/n]} * TOD_{i-[i/n]n}},\ i = 1, \cdots, nT \tag{23}$$

The total variation that is due to jumps is therefore given by

$$JV_t = RV_t - CV_t \tag{24}$$

with left and right jump tail variations defined as the part attributable to large negative and large positive jumps, respectively.

7.3 Option-Implied Skewness

The option-implied skewness is obtained using the approach of Bakshi, Kapadia, and Madan (2003). The basic idea is that the implied skewness can be written as a function of the current price of three securities that pay quadratic, cubic and quartic payoffs equal to the second, third, and fourth power of VIX futures log return, respectively. These payoffs can be further expressed as a linear combination of OTM option prices.

The time t prices of these three securities are given by

$$V_t(\tau) = \int_{F_t}^{\infty} \frac{2\left(1-\log(\frac{K}{F_t})\right)}{K^2} C_t(\tau,K)dK + \int_0^{F_t} \frac{2\left(1+\log(\frac{F_t}{K})\right)}{K^2} P_t(\tau,K)dK \tag{25}$$

$$\begin{aligned} W_t(\tau) &= \int_{F_t}^{\infty} \frac{6\log(\frac{K}{F_t}) - 3\left(\log(\frac{K}{F_t})\right)^2}{K^2} C_t(\tau,K)dK \\ &\quad - \int_0^{F_t} \frac{6\log(\frac{F_t}{K}) + 3\left(\log(\frac{F_t}{K})\right)^2}{K^2} P_t(\tau,K)dK \end{aligned} \tag{26}$$

and

$$\begin{aligned} X_t(\tau) &= \int_{F_t}^{\infty} \frac{12\left(\log(\frac{K}{F_t})\right)^2 - 4\left(\log(\frac{K}{F_t})\right)^3}{K^2} C_t(\tau,K)dK \\ &\quad + \int_0^{F_t} \frac{12\left(\log(\frac{F_t}{K})\right)^2 + 4\left(\log(\frac{F_t}{K})\right)^3}{K^2} P_t(\tau,K)dK \end{aligned} \tag{27}$$

where F_t is the VIX futures price. The implied skewness is then derived as

$$SKEW_t = \frac{\exp(r\tau)(W_t(\tau) - 3\mu_t(\tau)V_t(\tau)) + 2\mu_t^3(\tau)}{[\exp(r\tau)V_t(\tau) - \mu_t^2(\tau)]^{3/2}} \tag{28}$$

where r is the risk-free rate, $\mu_t(\tau)$ is defined as

$$\mu_t(\tau) = \exp(r\tau) - 1 - \frac{\exp(r\tau)}{2}V_t(\tau) - \frac{\exp(r\tau)}{6}W_t(\tau) - \frac{\exp(r\tau)}{24}X_t(\tau) \tag{29}$$

References

Andersen, T. G., O. Bondarenko, and M. T. Gonzalez-Perez (2015): "Exploring Return Dynamics via Corridor Implied Volatility," *Review of Financial Studies*, 28(10), 2902–2945.

Andersen, T. G., N. Fusari, and V. Todorov (2015): "The risk premia embedded in index options," *Journal of Financial Economics*, 117, 558–584.

Andersen, T. G., N. Fusari, and V. Todorov (2020): "The Pricing of Tail Risk and the

Equity Premium: Evidence From International Option Markets," *Journal of Business and Economic Statistics*, 38(3), 662–678.

Andersen, T. G., V. Todorov, and M. Ubukata (2021): "Tail Risk and Return Predictability for the Japanese Equity Market," *Journal of Econometrics*, 222(1), 344–363.

Baker, S. R., N. Bloom, and S. J. Davis (2016): "Measuring Economic Policy Uncertainty," *The Quarterly Journal of Economics*, 131(4), 1593–1636.

Bakshi, G. S., and N. Kapadia (2003): "Delta-Hedged Gains and the Negative Market Volatility Risk Premium," *Review of Financial Studies*, 16(2), 527–566.

Bakshi, G. S., N. Kapadia, and D. Madan (2003): "Stock return characteristics, skew laws, and the differential pricing of individual equity options," *Review of Financial Studies*, 16(1), 101–143.

Bardgett, C., E. Gourier, and M. Leippold (2019): "Inferring volatility dynamics and risk premia from the SP500 and VIX markets R," *Journal of Financial Economics*, 131(3), 593–618.

Barndorff-Nielsen, O. E., and N. Shephard (2002): "Econometric analysis of realized volatility and its use in estimating stochastic volatility models," *Journal of the Royal Statistical Society. Series B: Statistical Methodology*, 64, 253–280.

Bekaert, G., E. C. Engstrom, and N. R. Xu (2022): "The Time Variation in Risk Appetite and Uncertainty," *Management Science*, 68(6), 3975–4004.

Bollerslev, T., J. Marrone, L. Xu, and H. Zhou (2014): "Stock Return Predictability and Variance Risk Premia: Statistical Inference and International Evidence," *Journal of Financial and Quantitative Analysis*, 49(03), 633–661.

Bollerslev, T., G. Tauchen, and H. Zhou (2009): "Expected stock returns and variance risk premia," *Review of Financial Studies*, 22(11), 4463–4492.

Bollerslev, T., and V. Todorov (2011a): "Estimation of Jump Tails," *Econometrica*, 79(6), 1727–1783.

——— (2011b): "Tails, Fears, and Risk Premia," *Journal of Finance*, 66(6), 2165–2211.

——— (2014): "Time-varying jump tails," *Journal of Econometrics*, 183(2), 168–180.

Bollerslev, T., V. Todorov, and S. Z. Li (2013): "Jump tails, extreme dependencies, and the distribution of stock returns," *Journal of Econometrics*, 172(2), 307–324.

Bollerslev, T., V. Todorov, and L. Xu (2015): "Tail risk premia and return predictability," *Journal of Financial Economics*, 118(1), 113–134.

Britten-Jones, M., and A. Neuberger (2000): "Option Prices, Implied Price Processes, and Stochastic Volatility," *Journal of Finance*, 55(2), 839–866.

Cakmakli, C., and D. van Dijk (2016): "Getting the most out of macroeconomic information for predicting excess stock returns," *International Journal of Forecasting*, 32(3), 650–668.

Campbell, J. Y., and S. B. Thompson (2008): "Predicting Excess Stock Returns out of Sample: Can Anything Beat the Historical Average?," *Review of Financial Studies*, 21(4), 1509–1531.

Campbell, J. Y., and M. Yogo (2006): "Efficient tests of stock return predictability," *Journal of Financial Economics*, 81(1), 27–60.

Christoffersen, P., K. Jacobs, and C. Ornthanalai (2012): "Dynamic jump intensities and risk premiums: Evidence from SP500 returns and options," *Journal of Financial Economics*, 106(3), 447–472.

Clark, T. E., and K. D. West (2007): "Approximately normal tests for equal predictive accuracy in nested models," *Journal of Econometrics*, 138(1), 291–311.

Corsi, F. (2009): "A simple approximate long-memory model of realized volatility," *Journal of Financial Econometrics*, 7(2), 174–196.

Drechsler, I., and A. Yaron (2010): "What's Vol got to do with it," *Review of Financial Studies*, 24(1), 1–45.

Duan, J.-C., and J.-G. Simonato (1998): "Empirical martingale simulation for asset prices," *Management Science*, 44, 1218–1233.

Duan, J.-C., and C.-Y. Yeh (2010): "Jump and volatility risk premiums implied by VIX," *Journal of Economic Dynamics and Control*, 34, 2232–2244.

Ellwanger, R. (2017): "On the tail risk premium in the oil market," *Bank of Canada Working Paper*, pp. 7–46.

Huang, D., C. Schlag, I. Shaliastovich, and J. Thimme (2019): "Volatility-of-Volatility Risk," *Journal of Financial and Quantitative Analysis*, 54(6), 2423–2452.

Jiang, G. J., and Y. S. Tian (2005): "The model-free implied volatility and its information content," *The Review of Financial Studies*, 18, 1305–1342.

Kaeck, A. (2018): "Variance-of-variance risk premium," *Review of Finance*, 22(4), 1549–1579.

Kostakis, A., T. Magdalinos, and M. Stamatogiannis (2015): "Robust Econometric Inference for Stock Return Predictability," *The Review of Financial Studies*, 28(5), 1506–1553.

Li, J., and G. Zinna (2018): "The Variance Risk Premium: Components, Term Structures, and Stock Return Predictability," *Journal of Business and Economic Statistics*, 36(3), 411–425.

Li, Z., M. Izzeldin, and X. Yao (2020): "Return predictability of variance differences: A fractionally cointegrated approach," *Journal of Futures Markets*, 40(7), 1072–1089.

Magdalinos, T., and P. Phillips (2009): "Limit Theory for Cointegrated Systems with Moderately Integrated and Moderately Explosive Regressors," *Econometric Theory*, 25(2), 482–526.

Mencía, J., and E. Sentana (2013): "Valuation of VIX derivatives," *Journal of Financial Economics*, 108(2), 367–391.

Neely, C. J., D. E. Rapach, J. Tu, and G. Zhou (2014): "Forecasting the equity risk premium: The role of technical indicators," *Management Science*, 60(7), 1772–1791.

Newey, W. K., and K. D. West (1987): "A Simple Positive Semi-Definite, Heteroskedasticity and Autocorrelation Consistent Covariance Matrix," *Econometrica*, 55, 703–708.

Park, Y. H. (2015): "Volatility-of-volatility and tail risk hedging returns," *Journal of Financial Markets*, 26, 38–63.

——— (2016): "The effects of asymmetric volatility and jumps on the pricing of VIX derivatives," *Journal of Econometrics*, 192(1), 313–328.

Pesaran, M. H., and R. J. Smith (1994): "A generalized R2 criterion for regression models estimated by the instrumental variables method," *Econometrica: Journal of the Econometric Society*, 62(3), 705–710.

Pyun, S. (2019): "Variance risk in aggregate stock returns and time-varying return predictability," *Journal of Financial Economics*, 132(1), 150–174.

Rapach, D. E., J. K. Strauss, and G. Zhou (2010): "Out-of-sample equity premium prediction: Combination forecasts and links to the real economy," *Review of Financial Studies*, 23(2), 821–862.

Taylor, N. (2019): "Forecasting returns in the VIX futures market," *International Journal of Forecasting*, 35(4), 1193–1210.

YANG, B., W. LONG, L. PENG, AND Z. CAI (2020): "Testing the Predictability of U.S. Housing Price Index Returns Based on an IVX-AR Model," *Journal of the American Statistical Association*, 115(532), 1598–1619.

YUAN, P. (2021): "Time-Varying Skew in VIX Derivatives Pricing," *Management Science*.

Table 1

Simulation Results of Varying Jump Risk Premia. This table reports the mean values of $VVIX^2_{[t,t+\tau]}$ and $VVRP_{t,\tau}$ with different jump risk premia over different horizons. Numbers in parenthesis denote the changes of the values with respect to those in the case where no jump risk premia exist, i.e. $\phi_+ = \phi_- = 0$. For the purpose of comparison, upward (downward) jump risk premium is set as zero when the downward (upward) jump risk premium is varying.

$VVIX^2_{[t,t+\tau]}$													
Maturity (τ)	30	60	90	120	180	250	Maturity	30	60	90	120	180	250
$\phi_+ = \phi_- = 0$	0.998	0.711	0.514	0.439	0.304	0.273	$\phi_+ = \phi_- = 0$	0.998	0.711	0.514	0.439	0.304	0.273
$\phi_+ = 2$, $\phi_- = 0$	1.156	0.787	0.579	0.510	0.336	0.279	$\phi_+ = 0$, $\phi_- = 2$	1.091	0.783	0.569	0.467	0.341	0.269
	(0.158)	(0.106)	(0.126)	(0.161)	(0.106)	(0.022)		(0.093)	(0.100)	(0.107)	(0.063)	(0.122)	(-0.012)
$\phi_+ = 4$, $\phi_- = 0$	1.369	0.899	0.677	0.552	0.401	0.334	$\phi_+ = 0$, $\phi_- = 4$	1.148	0.852	0.604	0.508	0.358	0.296
	(0.371)	(0.264)	(0.317)	(0.257)	(0.317)	(0.224)		(0.150)	(0.197)	(0.175)	(0.157)	(0.178)	(0.084)
$\phi_+ = 6$, $\phi_- = 0$	1.523	0.977	0.738	0.609	0.444	0.388	$\phi_+ = 0$, $\phi_- = 6$	1.212	0.786	0.670	0.502	0.366	0.322
	(0.526)	(0.374)	(0.435)	(0.388)	(0.459)	(0.424)		(0.214)	(0.105)	(0.303)	(0.143)	(0.203)	(0.179)
$\phi_+ = 8$, $\phi_- = 0$	1.717	1.077	0.835	0.684	0.449	0.389	$\phi_+ = 0$, $\phi_- = 8$	1.264	0.919	0.646	0.555	0.395	0.321
	(0.719)	(0.514)	(0.624)	(0.559)	(0.478)	(0.426)		(0.266)	(0.292)	(0.256)	(0.264)	(0.298)	(0.177)
$\phi_+ = 10$, $\phi_- = 0$	1.877	1.237	0.905	0.732	0.543	0.382	$\phi_+ = 0$, $\phi_- = 10$	1.451	0.949	0.711	0.556	0.408	0.331
	(0.880)	(0.738)	(0.761)	(0.667)	(0.786)	(0.400)		(0.453)	(0.334)	(0.384)	(0.267)	(0.341)	(0.212)
$VVRP_{t,\tau}$													
Maturity (τ)	30	60	90	120	180	250	Maturity	30	60	90	120	180	250
$\phi_+ = \phi_- = 0$	0.224	0.529	0.774	0.852	1.081	1.179	$\phi_+ = \phi_- = 0$	0.224	0.529	0.774	0.852	1.081	1.179
$\phi_+ = 2$, $\phi_- = 0$	0.066	0.454	0.709	0.781	1.049	1.173	$\phi_+ = 0$, $\phi_- = 2$	0.131	0.458	0.719	0.824	1.044	1.182
	(-0.706)	(-0.142)	(-0.084)	(-0.083)	(-0.030)	(-0.005)		(-0.415)	(-0.135)	(-0.071)	(-0.032)	(-0.034)	(0.003)
$\phi_+ = 4$, $\phi_- = 0$	-0.147	0.342	0.611	0.739	0.985	1.118	$\phi_+ = 0$, $\phi_- = 4$	0.074	0.389	0.684	0.783	1.027	1.156
	(-1.658)	(-0.354)	(-0.211)	(-0.132)	(-0.089)	(-0.052)		(-0.670)	(-0.265)	(-0.117)	(-0.081)	(-0.050)	(-0.019)
$\phi_+ = 6$, $\phi_- = 0$	-0.301	0.263	0.550	0.681	0.942	1.063	$\phi_+ = 0$, $\phi_- = 6$	0.010	0.455	0.618	0.789	1.019	1.130
	(-2.347)	(-0.503)	(-0.289)	(-0.200)	(-0.129)	(-0.098)		(-0.956)	(-0.141)	(-0.201)	(-0.074)	(-0.057)	(-0.041)
$\phi_+ = 8$, $\phi_- = 0$	-0.495	0.163	0.453	0.607	0.936	1.063	$\phi_+ = 0$, $\phi_- = 8$	-0.042	0.322	0.642	0.736	0.990	1.130
	(-3.213)	(-0.691)	(-0.414)	(-0.288)	(-0.134)	(-0.099)		(-1.187)	(-0.392)	(-0.170)	(-0.136)	(-0.084)	(-0.041)
$\phi_+ = 10$, $\phi_- = 0$	-0.655	0.004	0.383	0.559	0.842	1.070	$\phi_+ = 0$, $\phi_- = 10$	-0.228	0.292	0.577	0.734	0.977	1.121
	(-3.930)	(-0.992)	(-0.505)	(-0.344)	(-0.221)	(-0.093)		(-2.022)	(-0.449)	(-0.255)	(-0.138)	(-0.096)	(-0.049)

Table 2

Simulation Results of the Jump Tail Measures. Panel A reports the mean values of the jump tail measure under the risk-neutral and physical measures as well as the rejection rate of the null hypothesis of $RJV^Q_{[t,t+30]} = LJV^Q_{[t,t+30]}$ ($RJV^P_{[t,t+30]} = LJV^P_{[t,t+30]}$). Panel B reports the averaged values of the adjusted R^2 for the regression $y_t = c + \beta x_t + \varepsilon_t$, where y_t refers to the 30-day or 180-day $VVRP$, or their difference as a measure of the slope of the $VVRP$ term structure, x_t denotes the jump tail under the risk-neutral measure, i.e. $RJV^Q_{[t,t+30]}$ or $LJV^Q_{[t,t+30]}$. Numbers in parentheses represent the percentage of simulation replications in which the coefficient estimate of β is significant at the 5% level. The corresponding values of the adjusted R^2 and the significance ratio for $VVIX^2$ are reported in Panel C.

Panel A: Jump Tail Measures

	Risk-Neutral Measure			Physical Measure		
	$RJV^Q_{[t,t+30]}$	$LJV^Q_{[t,t+30]}$	Rejection Rate	$RJV^P_{[t,t+30]}$	$LJV^P_{[t,t+30]}$	Rejection Rate
$\phi_+ = \phi_- = 0$	0.160	0.070	98%	0.028	0.027	6%
$\phi_+ = \phi_- = 2$	0.214	0.154	98%			
$\phi_+ = \phi_- = 4$	0.353	0.229	100%			
$\phi_+ = \phi_- = 6$	0.496	0.353	98%			

Panel B: Contribution to the $VVRP_{t,\tau}$ and its term structure

	$VVRP_{t,30}$		$VVRP_{t,180}$		$VVRP_{t,180} - VVRP_{t,30}$	
	$RJV^Q_{[t,t+30]}$	$LJV^Q_{[t,t+30]}$	$RJV^Q_{[t,t+30]}$	$LJV^Q_{[t,t+30]}$	$RJV^Q_{[t,t+30]}$	$LJV^Q_{[t,t+30]}$
$\phi_+ = \phi_- = 0$	0.013	0.003	0.003	0.002	0.015	0.005
	(33%)	(6%)	(9%)	(9%)	(39%)	(8%)
$\phi_+ = \phi_- = 2$	0.020	0.004	0.003	0.001	0.030	0.005
	(50%)	(13%)	(14%)	(8%)	(68%)	(16%)
$\phi_+ = \phi_- = 4$	0.029	0.008	0.002	0.003	0.047	0.013
	(67%)	(23%)	(7%)	(11%)	(78%)	(37%)
$\phi_+ = \phi_- = 6$	0.045	0.016	0.008	0.005	0.063	0.027
	(81%)	(46%)	(21%)	(19%)	(85%)	(58%)

Panel C: Contribution to the $VVIX^2_{[t,t+\tau]}$ and its term structure

	$VVIX^2_{[t,t+30]}$		$VVIX^2_{[t,t+180]}$		$VVIX^2_{[t,t+180]} - VVIX^2_{[t,t+30]}$	
	$RJV^Q_{[t,t+30]}$	$LJV^Q_{[t,t+30]}$	$RJV^Q_{[t,t+30]}$	$LJV^Q_{[t,t+30]}$	$RJV^Q_{[t,t+30]}$	$LJV^Q_{[t,t+30]}$
$\phi_+ = \phi_- = 0$	0.563	0.183	0.485	0.235	0.542	0.173
	(100%)	(97%)	(100%)	(100%)	(100%)	(100%)
$\phi_+ = \phi_- = 2$	0.609	0.242	0.456	0.283	0.598	0.229
	(100%)	(99%)	(100%)	(99%)	(100%)	(100%)
$\phi_+ = \phi_- = 4$	0.644	0.297	0.434	0.302	0.620	0.287
	(100%)	(100%)	(100%)	(100%)	(100%)	(100%)
$\phi_+ = \phi_- = 6$	0.649	0.369	0.429	0.327	0.621	0.352
	(100%)	(100%)	(100%)	(100%)	(100%)	(100%)

Table 3

Summary Statistics for VIX Returns. The table reports the summary statistics for delta-neutral option returns and VIX futures returns. The time span is Mar 2006 through Dec 2020 on a daily basis. The moneyness is defined as $k = K/F_t(\tau)$, where K is the strike price and $F_t(\tau)$ denotes the futures price.The t-statistics are testing the null hypothesis that returns are equal to zero. The $\% < 0$ column shows the proportion of data that is less than zero.

Moneyness	Maturity (days)	Mean (%)	t-stat.	Median (%)	%<0	Min.	Max.	Std.	AR(1)
Panel A: VIX Options									
OTM Put									
$0.8 < k < 0.9$	30	-1.457%	-5.685	-1.486%	81%	-0.097	0.085	0.026	0.209
	60	-2.045%	-4.814	-2.185%	75%	-0.091	0.084	0.031	0.126
$0.9 < k < 1.0$	30	-1.658%	-5.693	-1.563%	78%	-0.115	0.087	0.030	0.353
	60	-2.520%	-5.230	-2.292%	81%	-0.120	0.108	0.036	0.316
OTM Call									
$1.0 < k < 1.1$	30	-1.785%	-4.871	-1.681%	78%	-0.173	0.088	0.039	0.176
	60	-2.310%	-3.649	-1.838%	69%	-0.189	0.086	0.048	0.366
$1.1 < k < 1.2$	30	-1.871%	-4.747	-1.442%	80%	-0.188	0.114	0.042	0.239
	60	-2.415%	-3.705	-1.037%	72%	-0.182	0.079	0.050	0.366
Panel B: VIX Futures									
		-0.004%	-0.050	-0.498%	57%	-0.329	0.753	0.055	-0.083

Table 4

Summary Statistics of Predictor Variables. The sample period is from Mar 2006 until Dec 2020. All variables are annualized and reported in the original scale with the exception of MA_t, MOM_t and EPU_t. $VVIX_t^2$ denotes the risk-neutral variance implied by the VIX options with maturity of 30 days; $VVRP_t$ is measured as the difference between monthly RV_t and $VVIX_t^2$, where RV_t is the realized variance of VIX futures over a monthly period; $VVRPS_t$ ($VVIXS_t$) denotes the slope of the $VVRP_t$ ($VVIX_t^2$) term structure; ; $VVRP_t^n$ ($VVIX_t^{2n}$)denote the components of $VVRP_t$ ($VVIX_t^2$) that are associated with the normal sized price movements; RJV_t^Q denotes the right jump tail variation; P_t/E_t and P_t/D_t denote the price-earning ratio and the price-dividend ratio; $DFSP_t$ denotes the default spread (between Moody's BAA and AAA corporate bond spreads); $TMSP_t$ denotes the terms spread (between 10-year T-bond and the 3-month T-bill yields); MA_t refers to the moving average rule with $s = 2$ and $l = 9$ and MOM_t stands for the momentum indicator with $m = 12$ in the work of Neely et al. (2014); EPU_t denotes the economic policy uncertainty measure of Baker et al. (2016) and RA_t denotes the risk aversion index of Bekaert et al. (2022); TED_t denotes the TED spread; $SPREAD_t$ denotes the average relative bid-ask spread that is computed as the ratio of the difference between ask and bid quotes to the midpoint of the bid and ask quotes and $SKEW_t$ denotes the option-implied skewness of Bakshi et al. (2003).

	$VVRP_t$	$VVRP_t^n$	$VVRPS_t$	$VVIX_t^2$	$VVIX_t^{2n}$	$VVIXS_t$	RJV_t^Q	$log(P_t/E_t)$	$log(P_t/D_t)$	$DFSP_t$	$TMSP_t$	MA_t	MOM_t	RA_t	EPU_t	TED_t	$SPREAD_t$	$SKEW_t$
Summary Statistics																		
Mean	-0.164	-0.682	0.977	0.632	0.129	-0.256	0.511	3.104	3.908	0.011	0.016	0.388	0.530	0.031	130.842	0.005	24.213	1.392
Std. dev.	0.149	0.260	0.409	0.172	0.218	0.127	0.179	0.410	0.129	0.005	0.011	0.489	0.500	0.009	49.001	0.005	9.900	0.694
Skewness	-0.309	-0.446	-0.275	0.331	0.457	-0.182	0.726	2.511	-2.206	2.831	-0.097	0.460	-0.120	3.541	1.392	2.969	1.141	0.548
Kurtosis	3.461	3.919	2.667	3.535	4.332	3.889	4.727	10.030	9.326	12.235	2.050	1.211	1.015	17.215	5.898	12.749	4.365	4.307
AR(1)	0.222	0.592	0.774	0.172	0.153	-0.019	0.538	0.981	0.959	0.950	0.978	0.561	0.471	0.802	0.828	0.716	0.533	0.428
Correlation Matrix																		
$VVRP_t$	1.000	0.725	-0.281	-0.973	-0.537	0.836	-0.212	0.166	-0.038	-0.068	0.094	-0.072	-0.137	-0.204	-0.328	0.054	0.074	0.331
$VVRP_t^n$		1.000	-0.179	-0.682	0.180	0.442	-0.827	0.293	-0.262	0.123	0.128	0.086	-0.005	0.112	-0.299	0.234	0.150	0.034
$VVRPS_t$			1.000	0.275	0.180	-0.221	0.025	-0.403	0.511	-0.649	-0.265	-0.133	-0.229	-0.517	-0.384	-0.478	0.202	0.332
$VVIX_t^2$				1.000	0.589	-0.848	0.173	-0.160	0.030	0.078	-0.132	0.120	0.187	0.214	0.341	-0.025	-0.014	-0.369
$VVIX_t^{2n}$					1.000	-0.666	-0.694	0.113	-0.258	0.246	-0.010	0.236	0.223	0.424	0.121	0.218	0.116	-0.452
$VVIXS_t$						1.000	0.056	0.154	0.140	-0.166	-0.073	-0.137	-0.161	-0.276	-0.135	-0.097	0.062	0.430
RJV_t^Q							1.000	-0.281	0.341	-0.230	-0.105	-0.181	-0.106	-0.326	0.157	-0.287	-0.153	0.222
$log(P_t/E_t)$								1.000	-0.603	0.594	0.070	0.068	0.312	0.473	0.102	0.264	0.123	-0.301
$log(P_t/D_t)$									1.000	-0.870	-0.339	-0.251	-0.253	-0.732	-0.029	-0.559	0.065	0.344
$DFSP_t$										1.000	0.227	0.304	0.395	0.821	0.255	0.622	-0.045	-0.485
$TMSP_t$											1.000	-0.103	-0.207	0.249	-0.176	0.087	-0.564	0.041
MA_t												1.000	0.397	0.297	0.135	0.361	0.072	-0.293
MOM_t													1.000	0.319	0.286	0.320	0.145	-0.385
RA_t														1.000	0.342	0.587	-0.096	-0.471
EPU_t															1.000	-0.015	-0.063	-0.263
TED_t																1.000	0.014	-0.385
$SPREAD_t$																	1.000	-0.109
$SKEW_t$																		1.000

Table 5a

Monthly Regressions of the VIX Futures Returns. This table reports the in-sample predictive regression results of VIX futures returns over the monthly horizon. The sample period is Mar 2006 through Dec 2020. All variable definitions are identical to Table 4. To account for the variation in the regressors' degree of persistence, we follow the IVX approach of Kostakis et al. (2015) and report in the parentheses the statistics obtained from the Wald test under the null that the slope coefficient equals to zero. All coefficient estimates are scaled up by a factor of 100 for presentation purposes. *, ** and *** indicate statistical significance at 90%, 95% and 99% confidence levels, respectively.

	Simple										Multiple		
$VVRP_t$	0.184***										0.180***	0.166***	0.138***
	(14.530)										(12.727)	(11.852)	(7.263)
$VVIX_t^2$		-0.167***											
		(10.130)											
$log(P_t/E_t)$			-0.049								0.019		
			(1.257)								(0.103)		
$log(P_t/D_t)$				0.128***							0.241**		
				(8.099)							(4.361)		
$DFSP_t$					-0.105**						0.088		
					(5.955)						(0.734)		
$TMSP_t$						-0.022					0.039		
						(0.215)					(0.489)		
MA_t							-0.081*					-0.036	
							(3.397)					(0.474)	
MOM_t								-0.130***				-0.104**	
								(8.620)				(4.179)	
EPU_t									-0.130***				-0.042
									(7.536)				(0.598)
RA_t										-0.138***			-0.101**
										(10.190)			(4.348)
Adj.R^2	0.084	0.075	0.001	0.042	0.027	-0.004	0.014	0.044	0.042	0.051	0.110	0.113	0.102

Table 5b

Quarterly Regressions of the VIX Futures Returns. This table reports the in-sample predictive regression results of VIX futures returns over the quarterly horizon. The sample period is Mar 2006 through Dec 2020. All variable definitions are identical to Table 4. To account for the variation in the regressors' degree of persistence, we follow the IVX approach of Kostakis et al. (2015) and report in the parentheses the statistics obtained from the Wald test under the null that the slope coefficient equals to zero. All coefficient estimates are scaled up by a factor of 100 for presentation purposes. *, ** and *** indicate statistical significance at 90%, 95% and 99% confidence levels, respectively.

	Simple										Multiple		
$VVRP_t$	0.164***										0.143***	0.149***	0.108***
	(17.160)										(11.446)	(13.201)	(6.694)
$VVIX_t^2$		-0.110***											
		(10.190)											
$log(P_t/E_t)$			-0.049*								0.000		
			(2.861)								(0.036)		
$log(P_t/D_t)$				0.108***							0.137		
				(13.980)							(2.395)		
$DFSP_t$					-0.097***						0.025		
					(12.070)						(0.107)		
$TMSP_t$						-0.037					0.007		
						(1.394)					(0.042)		
MA_t							-0.056*					-0.048	
							(3.703)					(1.248)	
MOM_t								-0.041				-0.004	
								(1.871)				(0.008)	
EPU_t									-0.101***				-0.015
									(11.170)				(0.143)
RA_t										-0.118***			-0.110***
										(17.860)			(11.236)
Adj.R^2	0.135	0.074	0.010	0.073	0.059	0.003	0.015	0.005	0.062	0.090	0.180	0.132	0.190

Table 5c

Annual Regressions of the VIX Futures Returns. This table reports the in-sample predictive regression results of VIX futures returns over the annual horizon. The sample period is Mar 2006 through Dec 2020. All variable definitions are identical to Table 4. To account for the variation in the regressors' degree of persistence, we follow the IVX approach of Kostakis et al. (2015) and report in the parentheses the statistics obtained from the Wald test under the null that the slope coefficient equals to zero. All coefficient estimates are scaled up by a factor of 100 for presentation purposes. *, ** and *** indicate statistical significance at 90%, 95% and 99% confidence levels, respectively.

	Simple										Multiple		
$VVRP_t$	0.062***										0.033***	0.061***	0.040***
	(24.800)										(9.715)	(23.718)	(12.447)
$VVIX_t^2$		-0.049***											
		(11.240)											
$log(P_t/E_t)$			-0.024*								0.047**		
			(3.544)								(9.863)		
$log(P_t/D_t)$				0.079***							0.087***		
				(51.060)							(8.277)		
$DFSP_t$					-0.065***						-0.012		
					(33.530)						(0.260)		
$TMSP_t$						-0.072					-0.037***		
						(34.610)					(9.285)		
MA_t							-0.002					0.007	
							(0.025)					(0.244)	
MOM_t								-0.015				-0.017*	
								(1.314)				(1.594)	
EPU_t									-0.070***				-0.019
									(33.060)				(2.098)
RA_t										-0.072***			-0.057***
										(43.020)			(25.333)
Adj.R^2	0.144	0.081	0.015	0.239	0.161	0.195	-0.006	0.002	0.179	0.199	0.383	0.142	0.291

Table 6a

Monthly Regressions of the VIX Futures Returns: a special treatment of the right jump tail variation. This table reports the in-sample predictive regression results of VIX futures returns over the monthly horizon. The sample period is Mar 2006 through Dec 2020. $VVRPS_t^n$ denotes the components of $VVRPS_t$ that is associated with the normal sized price movements. Definitions of all the other variables are identical to Table 4. To account for the variation in the regressors' degree of persistence, we follow the IVX approach of Kostakis et al. (2015) and report in the parentheses the statistics obtained from the Wald test under the null that the slope coefficient equals to zero. All coefficient estimates are scaled up by a factor of 100 for presentation purposes. *, ** and *** indicate statistical significance at 90%, 95% and 99% confidence levels, respectively.

	Simple		Multiple					
$VVRP_t$	0.184***		0.199***					
	(14.530)		(16.651)					
$VVRPS_t$			0.101*					
			(3.228)					
$VVRP_t^n$		0.048		0.069	0.384***	0.403***	0.336***	0.290**
		(1.283)		(2.136)	(18.582)	(17.030)	(12.790)	(6.587)
$VVRPS_t^n$				0.080	0.107*	0.118	0.066	0.023
				(2.447)	(3.424)	(2.237)	(1.436)	(0.043)
RJV_t^Q					0.302***	0.277***	0.248***	0.243***
					(13.293)	(10.758)	(7.474)	(7.234)
$log(P_t/E_t)$						0.022		
						(0.135)		
$log(P_t/D_t)$						0.262**		
						(4.761)		
$DFSP_t$						0.175		
						(2.301)		
$TMSP_t$						0.059		
						(1.058)		
MA_t							-0.029	
							(0.269)	
MOM_t							-0.084	
							(2.560)	
EPU_t								-0.036
								(0.251)
RA_t								-0.102
								(1.762)
Adj.R^2	0.084	0.004	0.092	0.014	0.101	0.113	0.108	0.104

Table 6b

Quarterly Regressions of the VIX Futures Returns: a special treatment of the right jump tail variation. This table reports the in-sample predictive regression results of VIX futures returns over the quarterly horizon. The sample period is Mar 2006 through Dec 2020. All variable definitions are identical to Table 6a. To account for the variation in the regressors' degree of persistence, we follow the IVX approach of Kostakis et al. (2015) and report in the parentheses the statistics obtained from the Wald test under the null that the slope coefficient equals to zero. All coefficient estimates are scaled up by a factor of 100 for presentation purposes. *, ** and *** indicate statistical significance at 90%, 95% and 99% confidence levels, respectively.

	Simple		Multiple					
$VVRP_t$	0.164***		0.161***					
	(17.160)		(17.251)					
$VVRPS_t$			0.062*					
			(3.008)					
$VVRP_t^n$		0.062		0.085**	0.306***	0.267***	0.279***	0.169*
		(2.694)		(4.258)	(17.150)	(10.332)	(11.677)	(3.571)
$VVRPS_t^n$				0.064*	0.066*	0.009	0.059	-0.066
				(2.872)	(3.110)	(0.027)	(2.698)	(0.710)
RJV_t^Q					0.237***	0.195***	0.204***	0.140*
					(11.980)	(7.675)	(6.647)	(3.523)
$log(P_t/E_t)$						0.006		
						(0.016)		
$log(P_t/D_t)$						0.145		
						(2.412)		
$DFSP_t$						0.028		
						(0.112)		
$TMSP_t$						0.007		
						(0.032)		
MA_t							-0.053	
							(1.374)	
MOM_t							0.018	
							(0.186)	
EPU_t								-0.031
								(0.377)
RA_t								-0.177***
								(8.256)
Adj.R^2	0.135	0.023	0.129	0.034	0.132	0.168	0.125	0.212

Table 6c

Annual Regressions of the VIX Futures Returns: a special treatment of the right jump tail variation. This table reports the in-sample predictive regression results of VIX futures returns over the quarterly horizon. The sample period is Mar 2006 through Dec 2020. All variable definitions are identical to Table 6a. To account for the variation in the regressors' degree of persistence, we follow the IVX approach of Kostakis et al. (2015) and report in the parentheses the statistics obtained from the Wald test under the null that the slope coefficient equals to zero. All coefficient estimates are scaled up by a factor of 100 for presentation purposes. *, ** and *** indicate statistical significance at 90%, 95% and 99% confidence levels, respectively.

	Simple		Multiple					
$VVRP_t$	0.062***		0.070***					
	(24.800)		(33.010)					
$VVRPS_t$			0.045***					
			(10.620)					
$VVRP_t^n$		0.035***		0.054***	0.123***	0.050**	0.120***	0.057***
		(7.018)		(13.423)	(28.296)	(4.136)	(24.686)	(4.908)
$VVRPS_t^n$				0.043***	0.044***	-0.011	0.041***	-0.016
				(8.631)	(9.885)	(0.300)	(8.808)	(0.587)
RJV_t^Q					0.080***	0.034***	0.076***	0.036**
					(14.459)	(2.947)	(11.062)	(2.766)
$log(P_t/E_t)$						0.050**		
						(10.149)		
$log(P_t/D_t)$						0.093***		
						(8.305)		
$DFSP_t$						-0.019		
						(0.569)		
$TMSP_t$						-0.041***		
						(9.126)		
MA_t							0.004	
							(0.081)	
MOM_t							-0.011	
							(0.701)	
EPU_t								-0.023
								(2.324)
RA_t								-0.076***
								(18.706)
Adj.R^2	0.144	0.042	0.187	0.084	0.159	0.358	0.150	0.269

Table 7a

Predictive Regressions of Delta-Hedged Option Returns with Maturity of 30 Days. This table reports the predictive regression results of the delta-hedged option gains onto $VVRP_t$, $VVIX_t^2$ and other variables of interest. All variable definitions are identical to Table 4. A lagged dependent variable is included to correct for the serial corelation of the residuals. We present the coefficient estimates, the Newey-West $t-$ statistics with an optimal lag in parentheses, the Box-Pierce statistic with 6 lags (denoted Q_6), and the P-values for Q_6 in square brackets. All coefficient estimates are scaled up by a factor of 100 for presentation purposes. *, ** and *** indicate statistical significance at 90%, 95% and 99% confidence levels, respectively.

	[1.0, 1.1]											[1.1, 1.2]										
	Simple							Multiple				Simple							Multiple			
$VVRP_t$	0.460*											0.512*										
	(1.758)											(1.882)										
$VVIX_t^2$		-0.657**						-0.725***	-0.650**	-0.653**	-0.793***		-0.749***						-0.816***	-0.711**	-0.746**	-0.923***
		(-2.403)						(-2.830)	(-2.400)	(-2.407)	(-2.729)		(-3.099)						(-2.845)	(-2.462)	(-2.582)	(-3.194)
$SKEW_t$			-0.019					-0.232						0.058					-0.204			
			(-0.067)					(-0.821)						(0.280)					(-1.000)			
$SPREAD_t$				0.261					0.239						0.423*					0.326		
				(1.080)					(0.991)						(1.850)					(1.440)		
TED_t					0.319*					0.310						0.359**					0.351*	
					(1.905)					(1.648)						(2.268)					(1.854)	
EPU_t						0.084					0.202						0.278					0.503*
						(0.308)					(0.611)						(1.183)					(1.783)
RA_t							0.285				0.364							0.139				0.128
							(1.415)				(1.383)							(1.108)				(0.856)
Adj.R^2	0.041	0.045	0.010	0.014	0.018	0.010	0.016	0.044	0.044	0.048	0.052	0.040	0.057	0.004	0.018	0.016	0.011	0.006	0.055	0.060	0.063	0.074
Q_6	3.750	4.130	3.317	3.161	2.981	3.097	3.162	3.641	4.048	3.994	3.493	5.600	5.319	4.748	3.471	3.872	3.954	4.117	4.655	4.264	4.787	6.777
	[0.441]	[0.389]	[0.506]	[0.531]	[0.561]	[0.542]	[0.531]	[0.457]	[0.400]	[0.407]	[0.479]	[0.070]	[0.061]	[0.093]	[0.173]	[0.144]	[0.139]	[0.128]	[0.098]	[0.119]	[0.091]	[0.148]

Table 7b

Predictive Regressions of Delta-Hedged Option Returns with Maturity of 60 Days. This table reports the predictive regression results of the delta-hedged option gains onto $VVRP_t$, $VVIX_t^2$ and other variables of interest. All variable definitions are identical to Table 4. A lagged dependent variable is included to correct for the serial corelation of the residuals. We present the coefficient estimates, the Newey-West $t-$ statistics with an optimal lag in parentheses, the Box-Pierce statistic with 6 lags (denoted Q_6), and the P-values for Q_6 in square brackets. All coefficient estimates are scaled up by a factor of 100 for presentation purposes. *, ** and *** indicate statistical significance at 90%, 95% and 99% confidence levels, respectively.

	[1.0, 1.1]											[1.1, 1.2]										
	Simple							Multiple				Simple							Multiple			
$VVRP_t$	0.501											0.328										
	(1.417)											(0.852)										
$VVIX_t^2$		-0.652**						-0.791***	-0.645**	-0.653**	-0.900**		-0.550*						-0.769**	-0.653*	-0.558*	-0.857**
		(-2.149)						(-2.725)	(-2.075)	(-2.002)	(-2.578)		(-1.730)						(-2.376)	(-1.799)	(-1.683)	(-2.311)
$SKEW_t$			-0.038					-0.353						-0.195					-0.510*			
			(-0.129)					(-1.271)						(-0.633)					(-1.743)			
$SPREAD_t$				0.428					0.418						0.501					0.447		
				(1.304)					(1.321)						(1.352)					(1.232)		
TED_t					0.232					0.236						0.181					0.200	
					(1.029)					(0.994)						(0.798)					(0.920)	
EPU_t						0.612					0.873						0.725					0.978*
						(1.532)					(1.679)						(1.652)					(1.927)
RA_t							0.163				0.022							0.219				0.046
							(0.853)				(0.111)							(0.958)				(0.253)
Adj.R^2	0.204	0.197	0.174	0.183	0.176	0.193	0.175	0.197	0.201	0.195	0.223	0.179	0.186	0.174	0.181	0.173	0.195	0.174	0.191	0.187	0.182	0.215
Q_6	2.582	3.044	2.072	2.951	2.110	2.019	2.117	2.504	3.912	3.011	3.057	1.389	1.313	1.965	2.170	1.900	2.302	1.974	5.936	1.647	1.415	2.022
	[0.461]	[0.385]	[0.558]	[0.399]	[0.550]	[0.569]	[0.549]	[0.475]	[0.271]	[0.390]	[0.383]	[0.499]	[0.519]	[0.374]	[0.338]	[0.387]	[0.316]	[0.373]	[0.115]	[0.439]	[0.493]	[0.364]

Table 8a

Predictive Regressions of Delta-Hedged Option Returns with Maturity of 30 Days: a special treatment of the right jump tail variation. This table reports the predictive regression results of the delta-hedged option gains onto $VVIX_t^2$, $VVIX_t^{2n}$, $VVIXS_t$, $VVIXS_t^n$, RJV_t^Q and other variables of interest. $VVIXS_t^n$ denotes the component of $VVIXS_t$ that is stripped of the right jump tail variation. Definitions of all the other variables are identical to Table 4. A lagged dependent variable is included to correct for the serial corelation of the residuals. We present the coefficient estimates, the Newey-West $t-$ statistics with an optimal lag in parentheses, the Box-Pierce statistic with 6 lags (denoted Q_6), and the P-values for Q_6 in square brackets. All coefficient estimates are scaled up by a factor of 100 for presentation purposes. *, ** and *** indicate statistical significance at 90%, 95% and 99% confidence levels, respectively.

	[1.0, 1.1]									[1.1, 1.2]								
$VVIX_t^2$	-0.657**		-0.834**							-0.749***		-0.910***						
	(-2.403)		(-2.374)							(-3.099)		(-3.037)						
$VVIXS_t$			-0.211									-0.193						
			(-0.519)									(-0.578)						
$VVIX_t^{2n}$		-0.434*		-0.183	-1.329**	-1.472***	-1.391**	-1.213**	-1.752**		-0.516**		-0.267	-1.368***	-1.480***	-1.325***	-1.265***	-2.136***
		(-1.678)		(-0.861)	(-2.440)	(-2.637)	(-2.601)	(-2.293)	(-2.345)		(-2.091)		(-1.209)	(-2.999)	(-3.501)	(-3.323)	(-2.964)	(-3.390)
$VVIXS_t^n$				0.383	-0.314	-0.274	-0.359	-0.232	-0.526				0.376	-0.281	-0.252	-0.264	-0.215	-0.723
				(1.198)	(-0.729)	(-0.631)	(-0.791)	(-0.513)	(-0.957)				(1.138)	(-0.801)	(-0.717)	(-0.697)	(-0.601)	(-1.525)
RJV_t^Q					-1.000**	-1.003***	-1.001**	-0.831**	-1.225**					-0.954***	-0.954**	-0.858***	-0.745**	-1.566***
					(-2.453)	(-2.631)	(-2.507)	(-1.985)	(-2.192)					(-2.863)	(-3.337)	(-2.923)	(-2.398)	(-3.300)
$SKEW_t$						-0.352									-0.268			
						(-1.033)									(-1.042)			
$SPREAD_t$							0.255									0.327		
							(0.880)									(0.969)		
TED_t								0.329									0.448	
								(1.243)									(1.649)	
EPU_t									0.274									0.672*
									(0.637)									(1.940)
RA_t									0.414									0.109
									(1.180)									(0.522)
Adj.R^2	0.045	0.026	0.041	0.027	0.042	0.044	0.040	0.043	0.052	0.057	0.030	0.053	0.032	0.048	0.047	0.049	0.057	0.076
Q_6	4.130	2.727	4.372	2.740	3.478	2.678	3.242	3.066	2.476	5.319	4.616	5.706	4.320	5.213	3.958	3.967	4.153	3.555
	[0.389]	[0.604]	[0.358]	[0.602]	[0.481]	[0.613]	[0.518]	[0.547]	[0.649]	[0.070]	[0.099]	[0.058]	[0.115]	[0.074]	[0.138]	[0.138]	[0.125]	[0.169]

Table 8b

Predictive Regressions of Delta-Hedged Option Returns with Maturity of 60 Days: a special treatment of the right jump tail variation. This table reports the predictive regression results of the delta-hedged option gains onto $VVIX_t^2$, $VVIX_t^{2n}$, $VVIXS_t$, $VVIXS_t^n$, RJV_t^Q and other variables of interest. All variable definitions are identical to Table 8a. A lagged dependent variable is included to correct for the serial corelation of the residuals. We present the coefficient estimates, the Newey-West $t-$ statistics with an optimal lag in parentheses, the Box-Pierce statistic with 6 lags (denoted Q_6), and the P-values for Q_6 in square brackets. All coefficient estimates are scaled up by a factor of 100 for presentation purposes. *, ** and *** indicate statistical significance at 90%, 95% and 99% confidence levels, respectively.

	[1.0, 1.1]									[1.1, 1.2]								
$VVIX_t^2$	-0.652**		-1.054**							-0.550*		-1.019**						
	(-2.149)		(-2.310)							(-1.696)		(-2.277)						
$VVIXS_t$			-0.482									-0.546						
			(-1.160)									(-1.380)						
$VVIX_t^{2n}$		-0.660**		-0.701**	-1.916***	-2.148***	-2.089***	-1.808***	-3.160***		-0.502		-0.640*	-1.847**	-2.158***	-1.737**	-1.770**	-3.264***
		(-2.104)		(-1.985)	(-2.722)	(-3.106)	(-2.895)	(-2.657)	(-3.269)		(-1.553)		(-1.759)	(-2.596)	(-3.099)	(-2.370)	(-2.568)	(-3.376)
$VVIXS_t^n$				-0.065	-0.829*	-0.690	-0.972**	-0.745*	-1.584**				-0.214	-0.954*	-0.791*	-0.895*	-0.890*	-1.760***
				(-0.181)	(-1.744)	(-1.577)	(-2.234)	(-1.679)	(-2.454)				(-0.543)	(-1.974)	(-1.703)	(-1.755)	(-1.939)	(-2.693)
RJV_t^Q					-1.080**	-1.047**	-1.113**	-0.895*	-2.147***					-1.051**	-1.039**	-0.845*	-0.874*	-2.226***
					(-2.130)	(-2.257)	(-2.114)	(-1.811)	(-2.941)					(-2.179)	(-2.508)	(-1.650)	(-1.948)	(-3.450)
$SKEW_t$						-0.611									-0.752**			
						(-1.620)									(-2.019)			
$SPREAD_t$							0.550									0.554		
							(1.624)									(1.350)		
TED_t								0.378									0.414	
								(1.078)									(1.168)	
EPU_t									1.165**									1.266***
									(2.294)									(2.635)
RA_t									0.059									0.137
									(0.230)									(0.615)
Adj.R^2	0.197	0.199	0.195	0.194	0.204	0.212	0.214	0.205	0.251	0.186	0.189	0.184	0.184	0.192	0.204	0.197	0.192	0.243
Q_6	3.044	2.830	2.903	2.778	2.827	2.257	4.127	2.878	2.513	1.313	1.427	0.968	1.384	0.883	1.585	1.513	1.257	1.322
	[0.385]	[0.419]	[0.407]	[0.427]	[0.419]	[0.521]	[0.248]	[0.411]	[0.473]	[0.519]	[0.490]	[0.616]	[0.501]	[0.643]	[0.453]	[0.469]	[0.533]	[0.516]

Table 9

Out-of-Sample Forecasts of VIX Futures Returns. This table reports the out-of-sample forecasting results of the VIX futures returns. OOS R^2 measures the reduction in mean squared forecast error for the predictive regression forecast relative to the historical average; $t-$statistics is derived using the approach of Clark and West (2007) that helps examine the forecasting gains of the models of interest relative to the benchmark model; the CER gain for a mean-variance investor is the CER difference, defined as the difference between the CER of forecasts given by the model of interest and the benchmark model. The historical average VIX futures returns serve as the benchmark for Panel A and Model 3 is treated as the benchmark for Panel B. The highest values of OOS R^2 in Panel A and B are separately highlighted in bold. *, ** and *** indicate statistical significance at 90%, 95% and 99% confidence levels, respectively.

	horizon	1	2	3	4	5	6	7	8	9	10	11	12
Panel A	Model 1: $VVRP_t$												
	OOR^2	0.010	0.065	0.115	0.062	0.026	**0.037**	**0.041**	**0.091**	**0.074**	**-0.008**	**-0.026**	**-0.011**
	MSPE-adjusted	0.832	1.663**	1.788**	1.618*	1.223	1.500*	1.730**	2.156**	2.092**	1.527*	1.284*	1.423*
	CER gain (%)	-0.002	0.039	0.055	0.044	0.029	0.033	0.034	0.034	0.029	0.016	0.019	0.018
	Model 2: $VVRP_t^n$												
	OOR^2	-0.008	-0.041	0.002	-0.008	-0.027	-0.023	-0.014	0.004	0.005	-0.047	-0.059	-0.064
	MSPE-adjusted	-0.482	-1.587	0.452	0.041	-0.413	-0.161	0.358	0.867	1.034	0.389	0.176	0.130
	CER gain (%)	-0.065	-0.037	0.002	0.007	0.003	0.009	0.014	0.016	0.015	0.010	0.009	0.008
	Model 3: $VVRP_t^n + RJV_t^Q$												
	OOR^2	**0.073**	**0.148**	**0.189**	**0.093**	**0.057**	0.030	-0.003	0.027	-0.001	-0.067	-0.040	-0.034
	MSPE-adjusted	2.138**	2.220**	2.013**	2.001**	1.941**	1.769**	1.731**	2.055**	1.856**	1.405*	1.644**	1.568*
	CER gain (%)	0.120	0.164	0.127	0.074	0.045	0.038	0.032	0.031	0.023	0.011	0.021	0.019
Panel B	Model 4: $VVRP_t^n + RJV_t^Q + log(P_t/E_t) + log(P_t/D_t) + DFSP_t + TMSP_t$												
	OOR^2	0.023	0.065	0.114	0.041	**0.053**	**0.063**	**0.104**	**0.210**	**0.227**	**0.152**	**0.263**	**0.233**
	MSPE-adjusted	0.104	-0.202	0.167	0.347	1.084	1.634*	2.458***	2.975***	3.664***	3.795***	4.339***	3.814***
	CER gain (%)	-0.064	-0.012	0.001	0.017	0.008	0.012	0.019	0.017	0.019	0.018	0.011	0.008
	Model 5: $VVRP_t^n + RJV_t^Q + MA_t + MOM_t$												
	OOR^2	**0.062**	**0.127**	0.164	0.086	0.033	0.011	-0.012	0.009	0.028	-0.042	0.012	-0.014
	MSPE-adjusted	-0.025	0.167	0.564	1.003	0.683	0.688	0.657	0.384	1.460*	1.168	1.736**	1.062
	CER gain (%)	-0.246	0.017	0.052	0.059	0.049	0.047	0.026	0.012	0.006	0.006	0.003	0.004
	Model 6: $VVRP_t^n + RJV_t^Q + EPU_t + RA_t$												
	OOR^2	0.053	0.119	**0.189**	**0.113**	0.043	0.034	0.017	0.079	0.107	0.025	0.008	0.022
	MSPE-adjusted	0.376	0.367	0.945	1.270	1.003	1.517*	2.215**	3.890***	4.251***	3.395***	2.452***	2.230***
	CER gain (%)	-0.074	-0.001	0.023	0.017	0.004	0.003	0.002	-0.001	0.001	0.004	0.000	0.001

Figure 1

$VVIX^2_{[t,t+\tau]}$ and $VVRP_{t,u}$ with Varying Jump Risk Premia and over Different Maturities. The figure provides a heat map showing values of $VVIX^2_{[t,t+\tau]}$ and $VVRP_{t,u}$ for different jump risk premia and maturities. For better comparison, ϕ_+ (ϕ_-) is set as zero when the value of ϕ_- (ϕ_+) is varying.

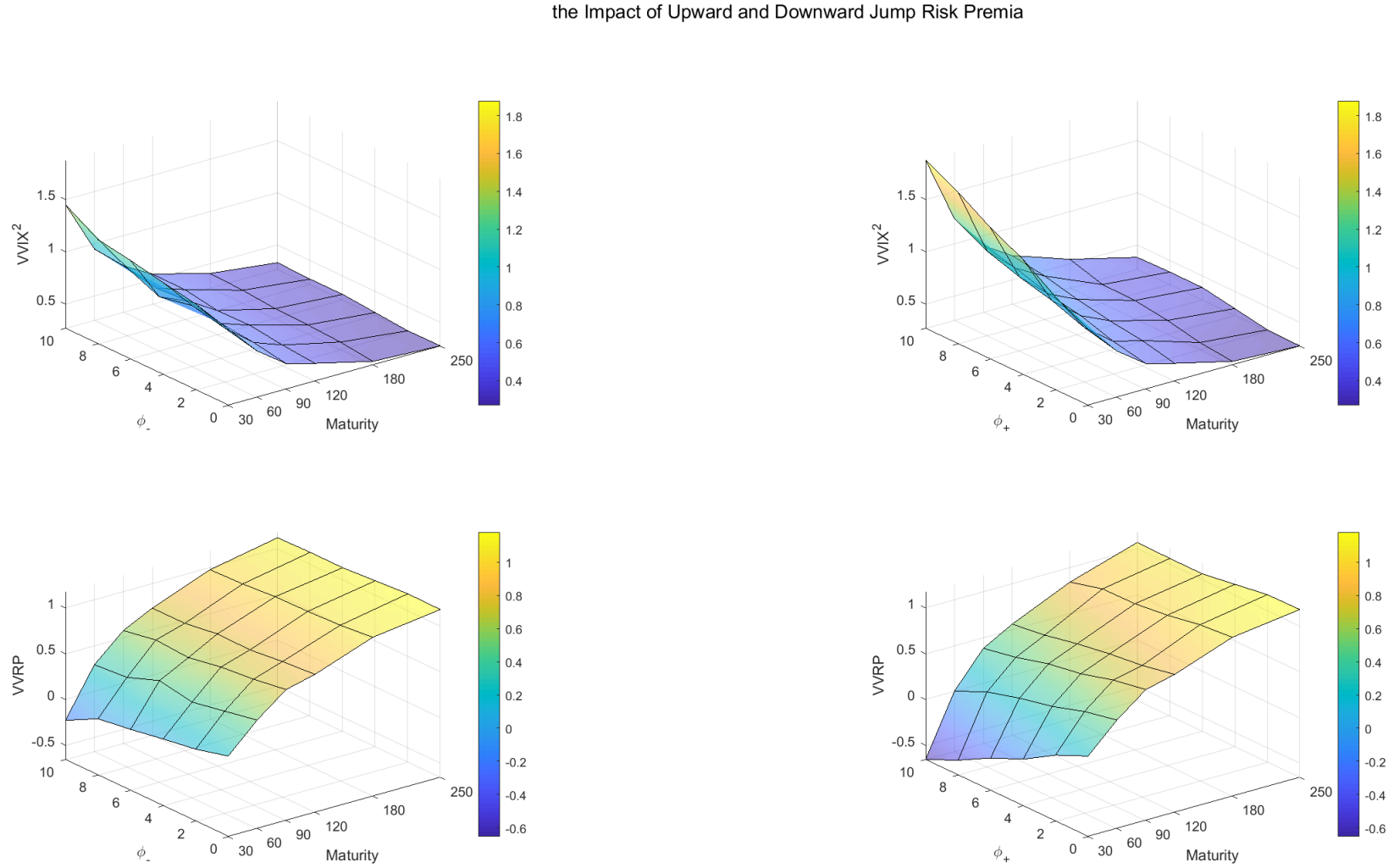

Figure 2

Predictor Variables. All the measures are plotted at a monthly frequency and cover the period from Mar 2006 to Dec 2020. The monthly measures are reported in annualized squared form with the single exception of EPU_t.

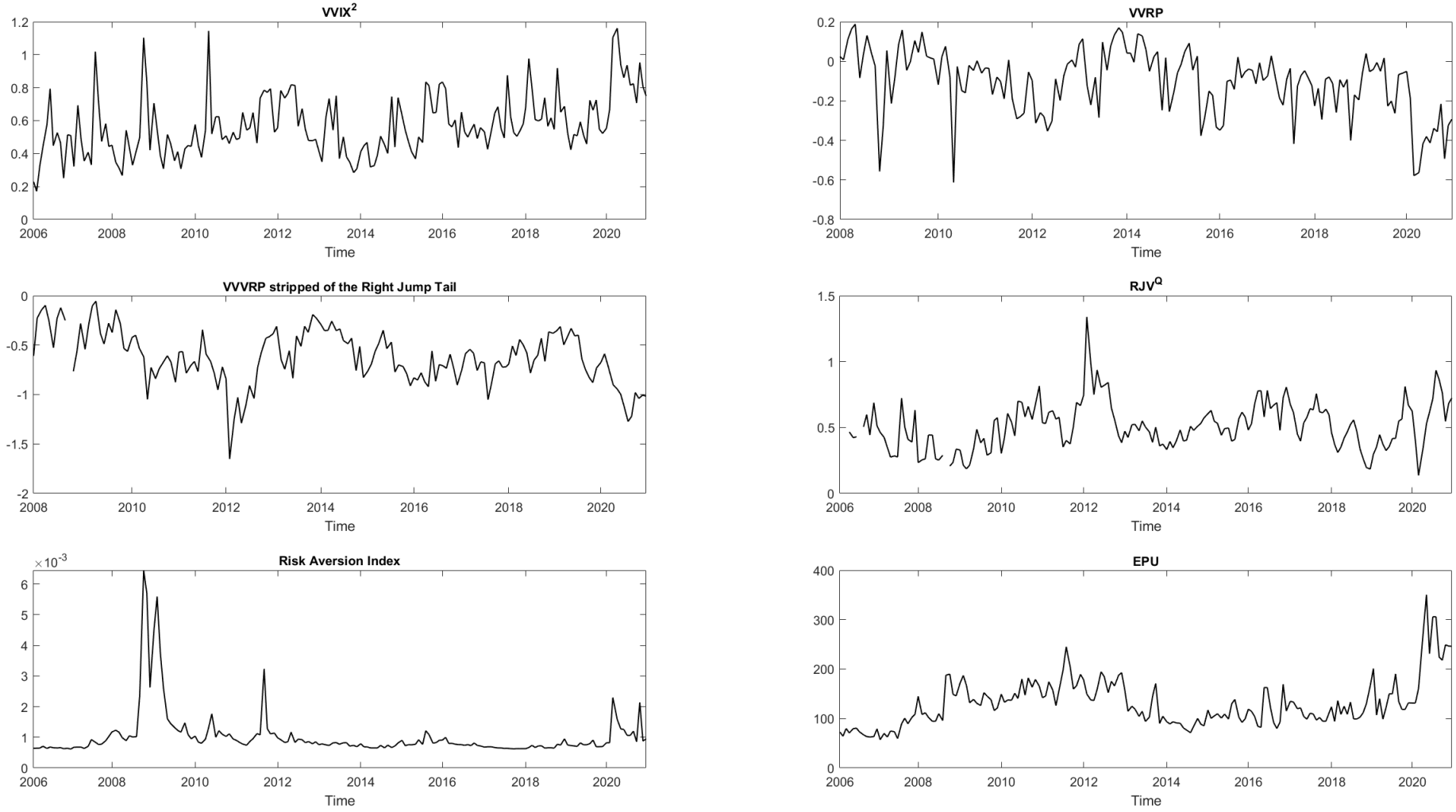

Figure 3
Volatility-of-Volatility Measures. The figure shows the time series of volatility-of-volatility measures. The blue line represents the measure calculated using VIX options and the black line represents the official VVIX index published by the CBOE in 2012. The official index is back-filled until 2006.

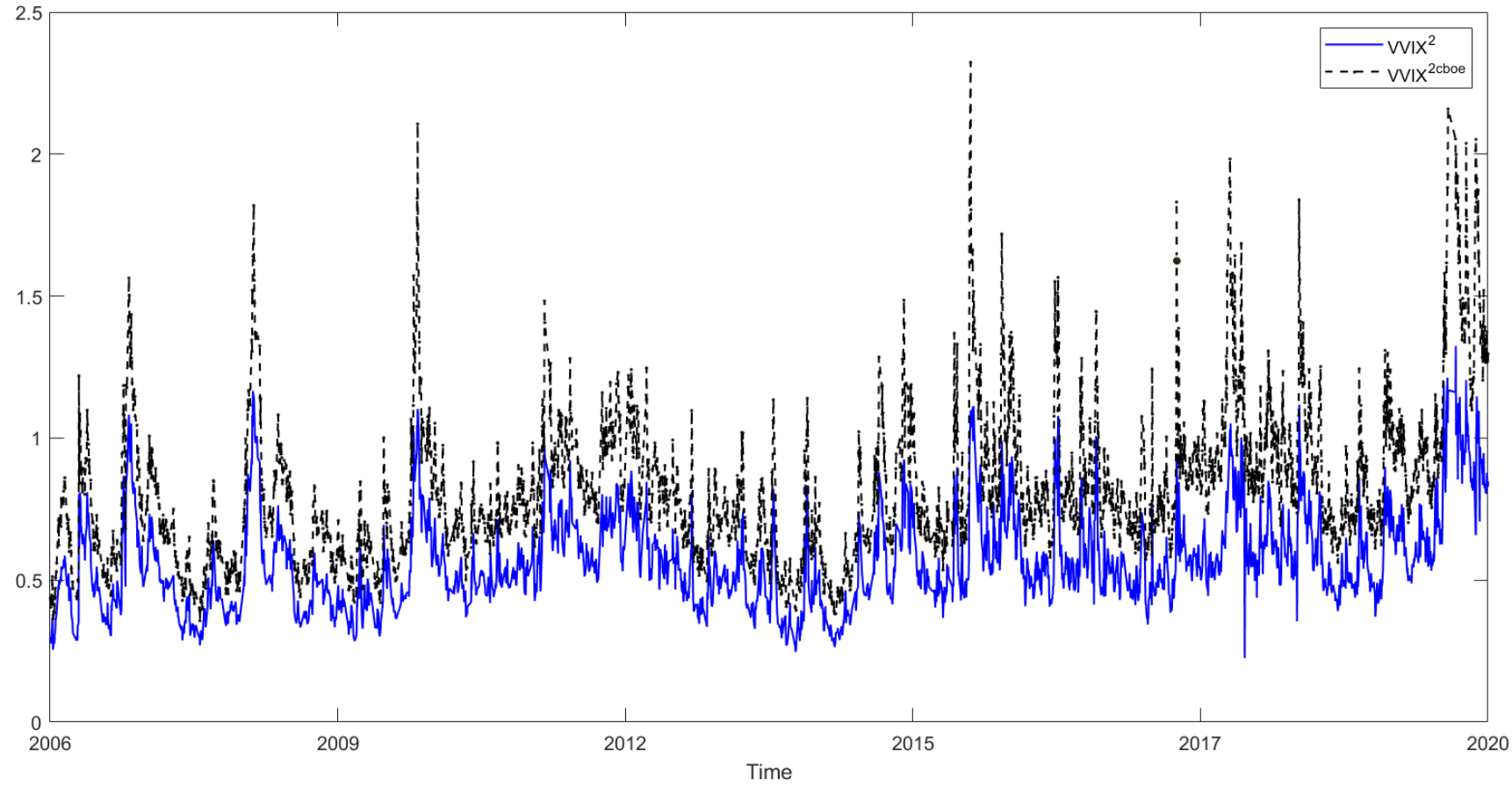

Figure 4

Realized Measures based on the VIX Futures High-Frequency Data. The upper panel depicts the time series of the daily realized variance and the continuous variation of the VIX and the lower panel presents the time series of the right and left jump tail variations under the physical measure.

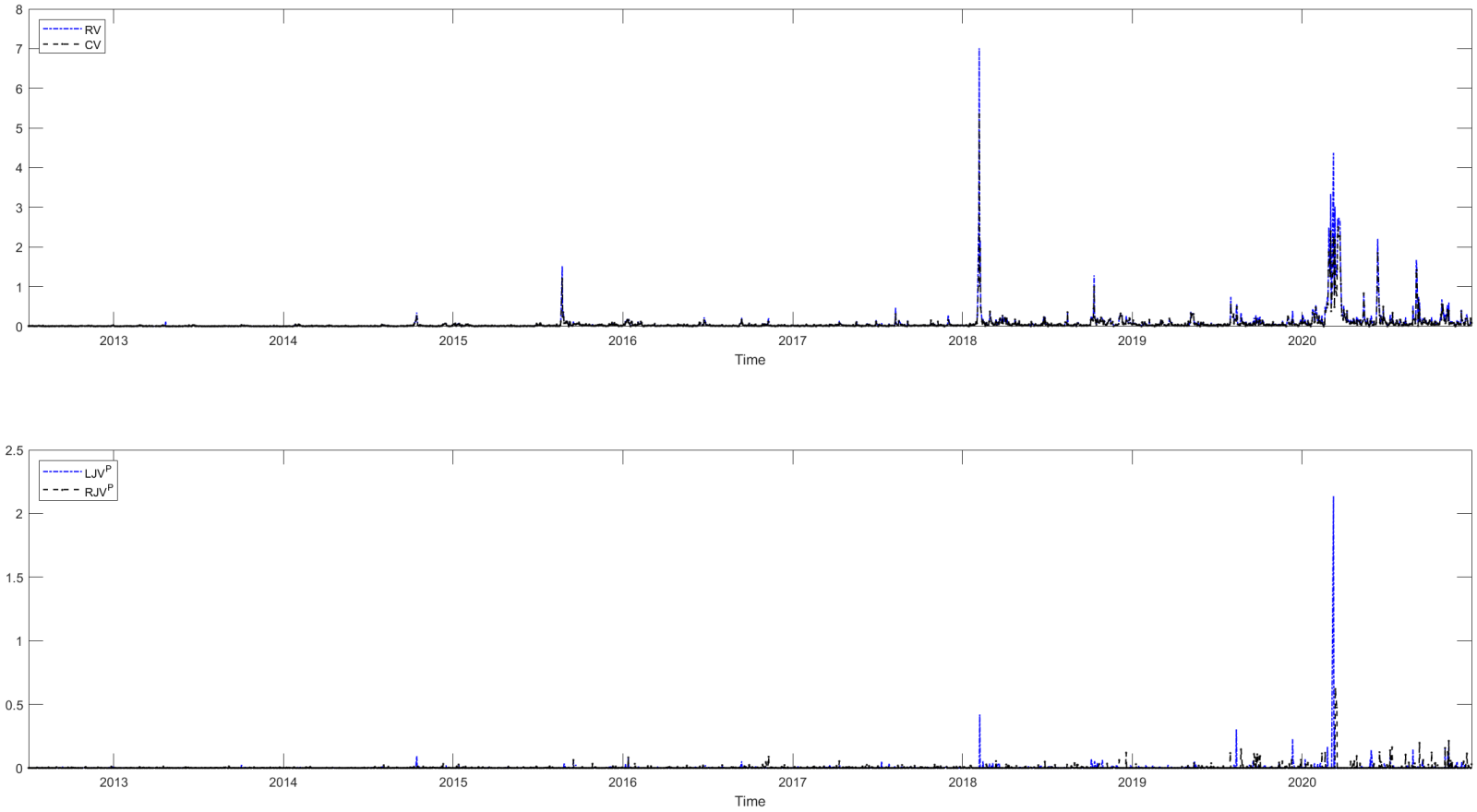

Figure 5

VIX Futures Return Predictability based on the CBOE VVIX Index and the VIX Futures High-Frequency Data. The figure depicts the adjusted R^2 from predictive regressions for the returns on VIX using $VVRP_t$, $VVIX_t^2$,the slope of $VVRP_t$ term structure and their components stripped of the right jump tail variation.